Interactions, structure, and elasticity in particulate gels

Eric M. Furst
Department of Chemical & Biomolecular Engineering
Allan P. Colburn Laboratory
University of Delaware

The University of Texas at Austin
Center for Dynamics and Control of Materials ++
April 26, 2023

Acknowledgments

Dr. Kathryn Whitaker
Dow

Prof. Lilian Hsiao
NCSU

Dr. Zsigmond Varga

Prof. Michael Solomon
Michigan

Prof. James Swan
MIT
(1982-2021)

International Fine Particles
Research Institute

NSF CBET-1235955

Colloidal gels

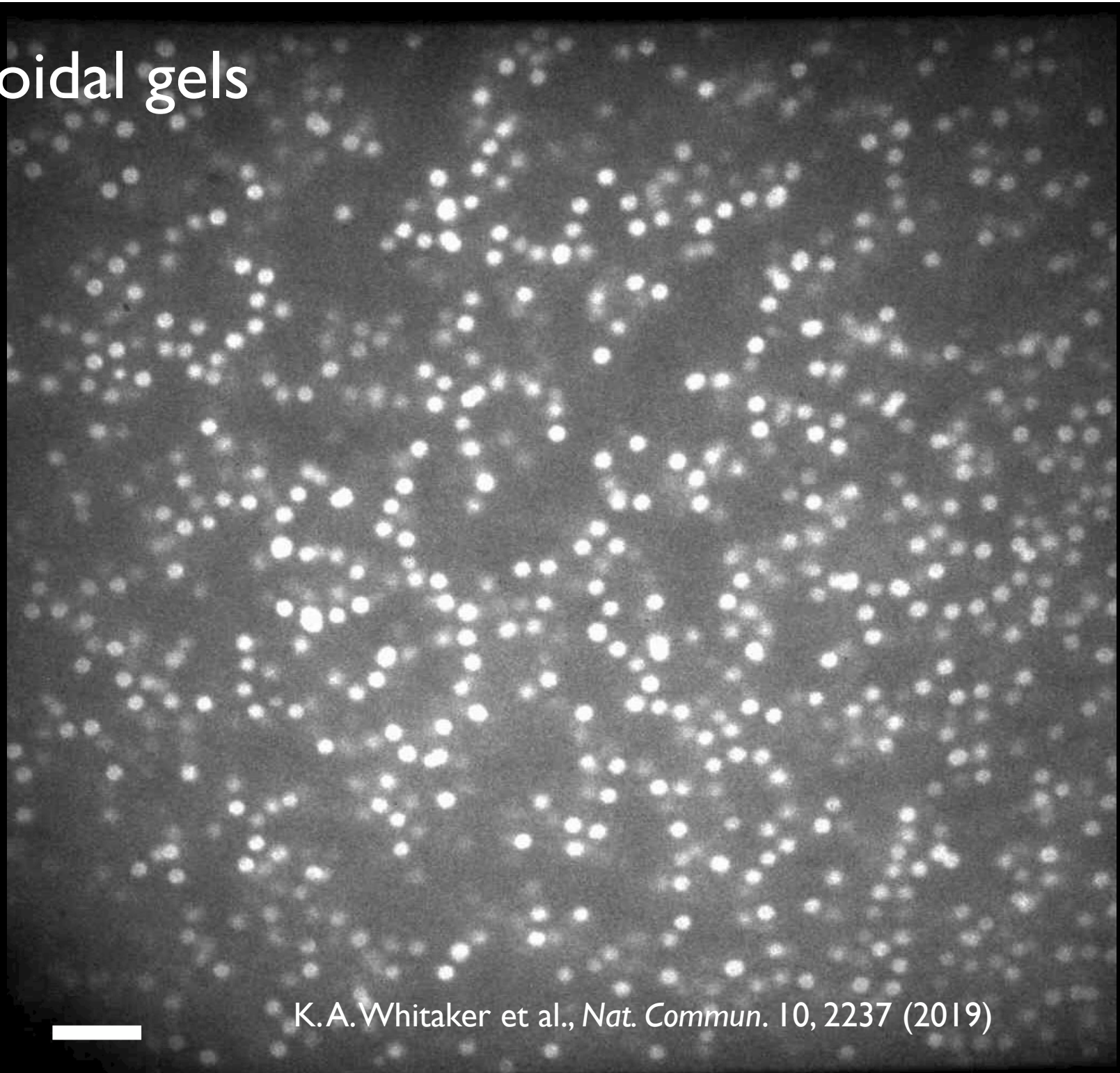

K. A. Whitaker et al., *Nat. Commun.* 10, 2237 (2019)

Colloid phase diagram with attraction

Gast, Hall, and Russel., *J. Colloid Interface Sci.*, 96, 251 (1983)
Lekkerkerker, Poon, Pusey, Stroobants, and Warren, *Europhys. Lett.* 20, 559–564 (1992)
Miller and Frenkel. *Phys. Rev. Lett.* 90, 135702 (2003)

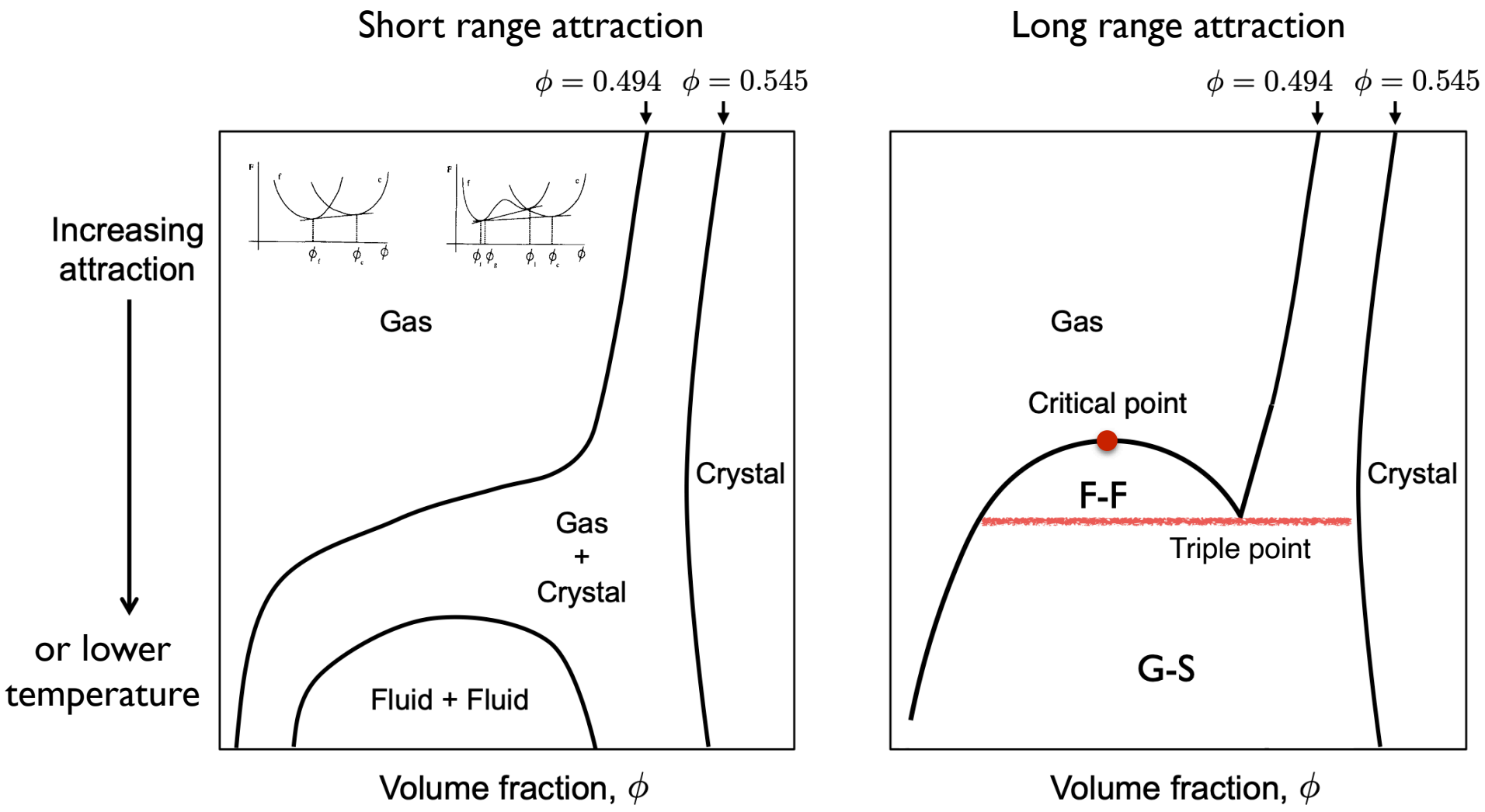

Vol 453|22 May 2008|doi:10.1038/nature06931 nature

LETTERS

Gelation of particles with short-range attraction

Peter J. Lu[1], Emanuela Zaccarelli[3,4], Fabio Ciulla[3], Andrew B. Schofield[5], Francesco Sciortino[3,4] & David A. Weitz[1,2]

Nanoscale or colloidal particles are important in many realms of science and technology. They can dramatically change the properties of materials, imparting solid-like behaviour to a wide variety of complex fluids[1,2]. This behaviour arises when particles aggregate to form mesoscopic clusters and networks. The essential component leading to aggregation is an interparticle attraction, which can be generated by many physical and chemical mechanisms. In the limit of irreversible aggregation, infinitely strong interparticle bonds lead to diffusion-limited cluster aggregation[3] (DLCA). This is understood as a purely kinetic phenomenon that can form solid-like gels at arbitrarily low particle volume fraction[4,5]. Far more important technologically are systems with weaker attractions, where gel formation requires higher volume fractions. Numerous scenarios for gelation have been proposed, including DLCA[6], kinetic or dynamic arrest[4,7–10], phase separation[5,6,11–16], percolation[4,12,17,18] and jamming[8]. No consensus has emerged and, despite its ubiquity and significance, gelation is far from understood—even the location of the gelation phase boundary is not agreed on[5]. Here we report experiments showing that gelation of spherical particles with isotropic, short-range attractions is initiated by spinodal decomposition; this thermodynamic instability triggers the formation of density fluctuations, leading to spanning clusters that dynamically arrest to create a gel. This simple picture of gelation does not depend on microscopic system-specific details, and should thus apply broadly to any particle system with short-range attractions. Our results suggest that gelation—often considered a purely kinetic phenomenon[4,8–10]—is in fact a direct consequence of equilibrium liquid–gas phase separation[5,13–15]. Without exception, we observe gelation in all of our samples predicted by theory and simulation to phase-separate; this suggests that it is phase separation, not percolation[12], that corresponds to gelation in models for attractive spheres.

Gelation occurs in a wide range of systems where particles attract each other[2,5–8,11,12,15–18]. When this attraction is infinitely strong, particles form permanent bonds and grow as fractal clusters that, in turn, bond irreversibly, and can ultimately span the system as a solid-like gel, even as particle volume fraction ϕ tends to zero (refs 4, 5, 12, 19). This DLCA limit occurs in many colloidal systems where the interparticle attraction strength, U, is much larger than the thermal energy k_BT (refs 4, 5, 12); examples include gold[3,20], silica[3], polymeric lattices[3,6,19], calcium carbonate[21], alumina[2] and silicon carbide[2]. Because bonds once formed never break, DLCA is governed entirely by diffusion; it has thus been considered a purely kinetic phenomenon[3]. Other mechanisms can cause kinetic arrest at far higher ϕ (ref. 5). Above $\phi \approx 0.58$, particles can arrest because of crowding to form repulsive glasses, even when $U = 0$; weakly attractive particles can form attractive glasses at lower ϕ (ref. 5). Because glasses and DLCA are observed in the same experimental systems, they have been linked within unified pictures of kinetic arrest[4,7,9,10] or jamming[8].

More generally, the onset of gelation can be parameterized by three quantities, namely ϕ, U/k_BT and ξ. The last is the range of the attractive potential in units of a, the particle radius[4,22]. These three parameters define a three-dimensional state diagram in which a gelation surface demarcates the well-defined boundary between liquid-like and solid-like behaviour. Many important attraction mechanisms that drive gelation are short-range ($\xi < 0.1$), including van der Waals forces[8,16,21], surface chemistry[2,17,18], hydrophobic effects[7] and some depletion interactions[9,15,23]. Numerous explanations have been advanced for gelation in this small-ξ limit to predict the fluid–solid boundary in the U–ϕ plane. Non-equilibrium, kinetics-based models have extended the DLCA model to lower U/k_BT by treating bond breakage probabilistically[6,12,20]; have connected the gelation boundary to the percolation threshold[4,12,17,18]; and have extended the glass transition to lower ϕ with mode-coupling theory applied to local arrest of individual particles[9], to arrest of clusters[4], and in concert with microscopic modelling of the interparticle attractive potential[23]. Thermodynamic models consider gelation initiated by fluid–crystal[11], liquid–gas[6,14,15], or polymer-like 'viscoelastic'[16] phase separation, which may arrest owing to percolation[12] or a glass transition[4]. These models make strikingly disparate predictions: there is no agreement on either the gelation mechanism, or the location of the gelation boundary[5,12,23].

Here we explore gelation experimentally with a widely-used model colloid–polymer system[6,11,22], where U/k_BT and ξ are controlled by the polymer size and free-volume concentration c_p, but in a fashion that is not precisely known. Fixing $\phi = 0.045 \pm 0.005$ and $\xi = 0.059$, we mix samples at various c_p; we summarize the samples studied by plotting their values of c_p, normalized by the polymer overlap concentration c_p^*, in the phase diagrams shown in Fig. 1a, b. We eliminate gravitational sedimentation on multiple-day timescales by meticulously matching the colloid and solvent densities to within $<10^{-4}$. After breaking up particle aggregates by shearing, we observe sample evolution with a high-speed confocal microscope[24].

We observe two phases. In samples with low c_p, below the experimental gelation boundary c_p^g, we observe a fluid of many clusters that is stable for days; we show a full three-dimensional image of these clusters in the fluid phase for a sample with $c_p = 3.20 \pm 0.03\ \mathrm{mg\,ml^{-1}}$, the closest fluid-phase value below c_p^g, in Fig. 1c and in Supplementary Video 1. By contrast, in samples with $c_p > c_p^g$, particles aggregate immediately into clusters, which in turn form a network that spans the macroscopic sample. This network subsequently arrests to create a gel, which we illustrate for a sample with $c_p = 3.31 \pm 0.03\ \mathrm{mg\,ml^{-1}}$, the closest gel-phase value above c_p^g, in Fig. 1d and in Supplementary Video 2. The gel undergoes no major structural rearrangement for days, even though it exchanges particles with a dilute gas, shown in Supplementary Video 3. These phases are separated by a very sharp boundary: the gel and fluid illustrated differ in c_p by only a few per cent. Our observation of only these two dramatically different phases contrasts findings of more complex phase behaviour in non-buoyancy-matched systems, where sedimentation can shift or obscure the observed phase boundaries[6,9,12,15,21].

[1]Department of Physics, [2]SEAS, Harvard University, Cambridge, Massachusetts 02138, USA. [3]Dipartimento di Fisica, [4]CNR-INFM-SOFT, Università di Roma La Sapienza, Piazzale A. Moro 2, 00185 Roma, Italy. [5]The School of Physics, University of Edinburgh, Edinburgh EH9 3JZ, UK.

boundary is not agreed on[5]. Here we report experiments showing that gelation of spherical particles with isotropic, short-range attractions is initiated by spinodal decomposition; this thermodynamic instability triggers the formation of density fluctuations, leading to spanning clusters that dynamically arrest to create a gel. This simple picture of gelation does not depend on microscopic system-specific details, and should thus apply broadly to any particle system with short-range attractions. Our results suggest that gelation—often considered a purely kinetic phenomenon[4,8–10]—is in fact a direct consequence of equilibrium liquid–gas phase separation[5,13–15]. Without exception, we observe gelation in all of our samples predicted by theory and simulation to phase-separate; this suggests that it is phase separation, not percolation[12], that corresponds to gelation in models for attractive spheres.

P. J. Lu, E. Zaccarelli, F. Ciulla, A. B. Schofield, F. Sciortino, and D. A. Weitz, *Nature* 453, 499 (2008).

Some gel lines from the literature

Baxter temperature

$$\tau_B = \left(\frac{2a+\Delta}{12\Delta}\right) e^{-\epsilon/kT}$$

Baxter, R. J., J.Chem. Phys. 49, 2770 (1968)

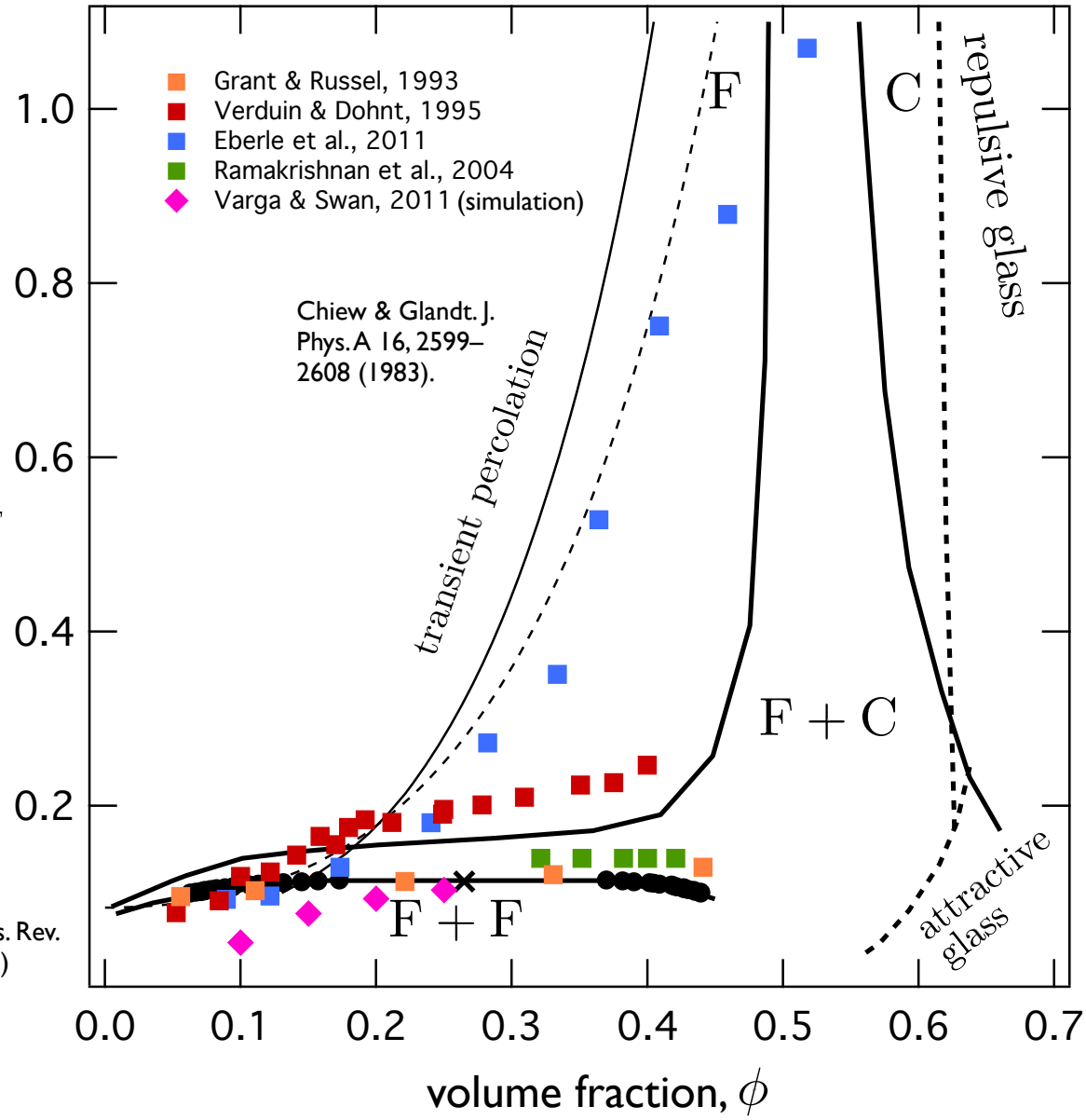

Miller and Frenkel. Phys. Rev. Lett. 90, 135702 (2003)

Pusey and van Megan, Phys. Rev. Lett. 59, 2083-2086 (1987)

Foffi et al. J Phys-Condens Mat 16, S3791-S3806 (2004)

Sciortino et al. Phys. Rev. Lett, 91, 268301 (2003)

Pham et al. Science 296, 104-106 (2002)

Strong attraction – flocs and fractal aggregates

Phase diagram
short range attraction

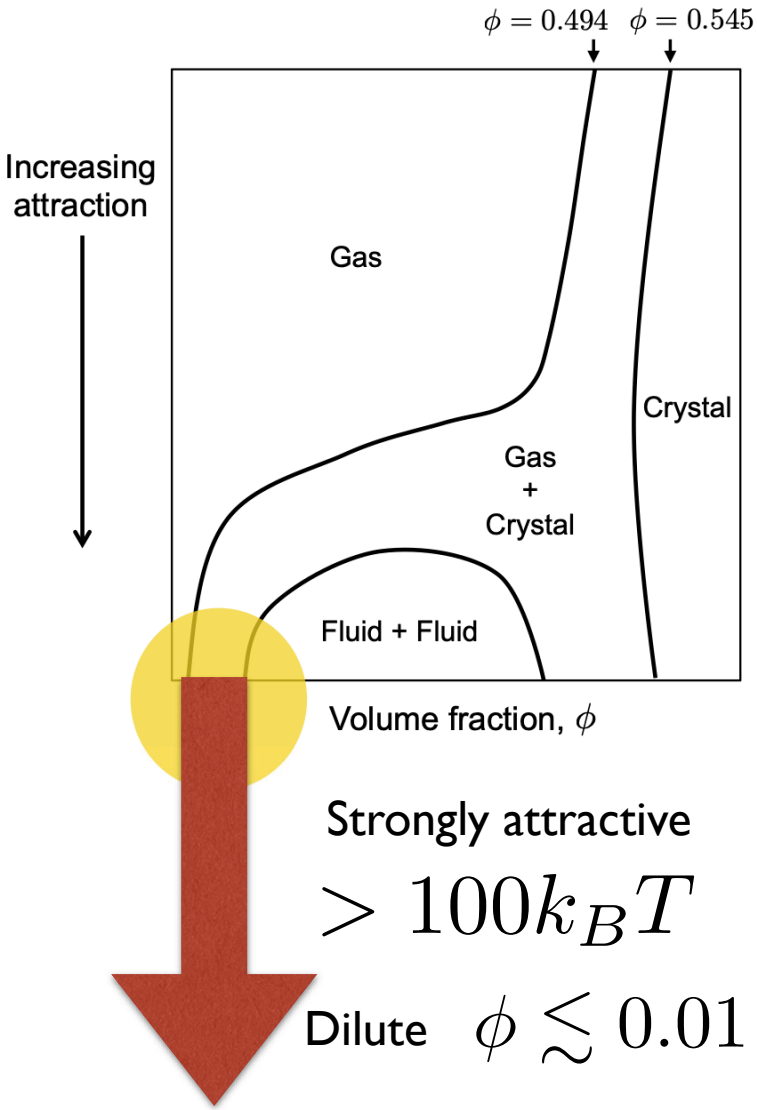

Strongly attractive

$> 100 k_B T$

Dilute $\phi \lesssim 0.01$

7.2nm Au particles

D. Weitz and M. Oliveria, Phys. Rev. Lett. 52, 1433 (1984).
D. Weitz, J. Huang, M. Lin, and J. Sung, Phys. Rev. Lett. 53, 1657 (1984).

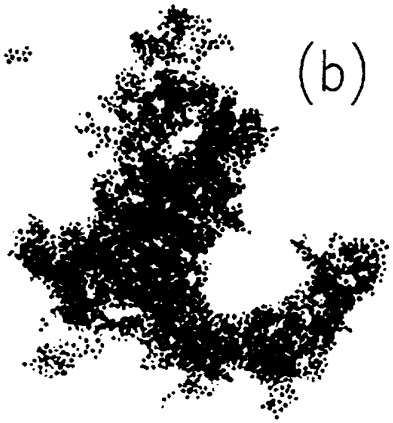

$$\xi \sim a k^{d_f}$$

d_f *Fractal dimension*

Diffusion limited

$d_f \approx 1.7 - 1.8$

Reaction limited

$d_f \approx 2.0 - 2.2$

"Cluster gels"

Lower attraction, higher density, central interactions

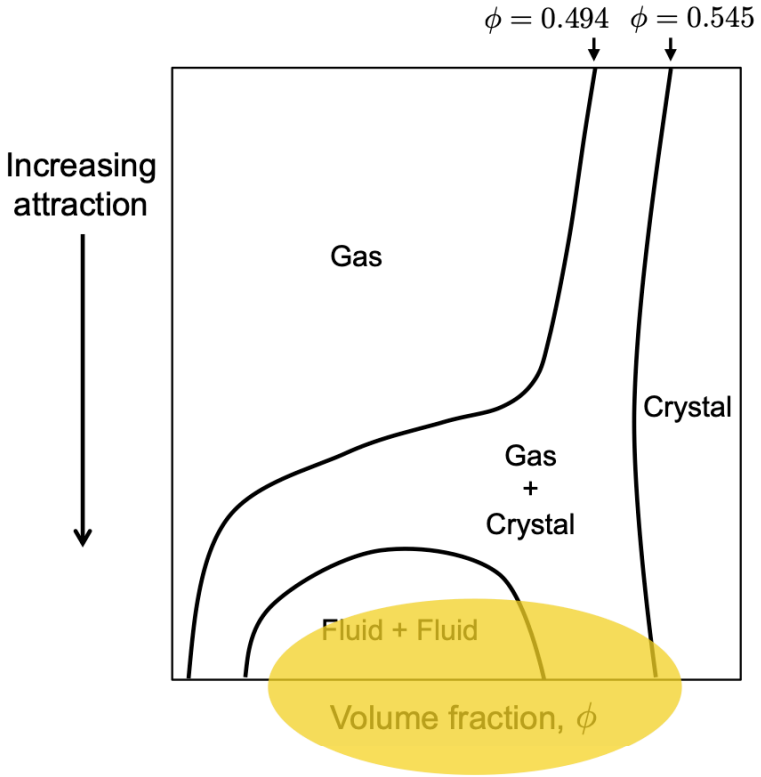

- Ramakrishnan, S.; Chen, Y.-L.; Schweizer, K. S.; Zukoski, C. F. *Phys. Rev. E* 70, 40401 (2004).
- N. Koumakis, G. Petekidis, *Soft Matter* 7, 2456 (2011).
- P. J. Lu, et al., *Nature* 453, 499 (2008).
- C. J. Dibble, M. Kogan, M. J. Solomon, *Phys. Rev. E* 74, 41403 (2006).

More weakly attractive

$$\sim 5 - 20 k_B T$$

More concentrated $\phi \sim 0.1 - 0.4$

Not fractal

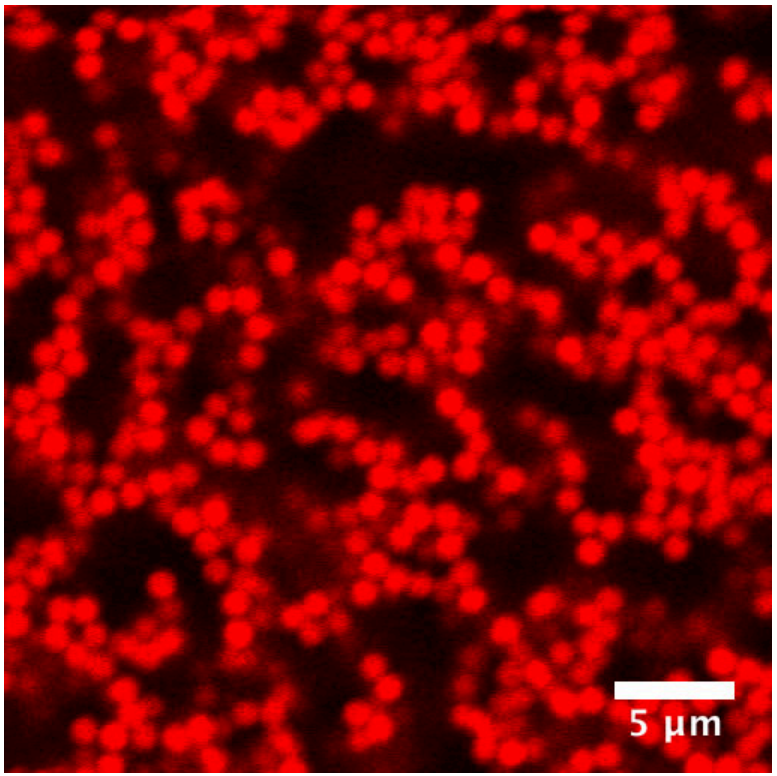

Elasticity, yield stress, viscosity

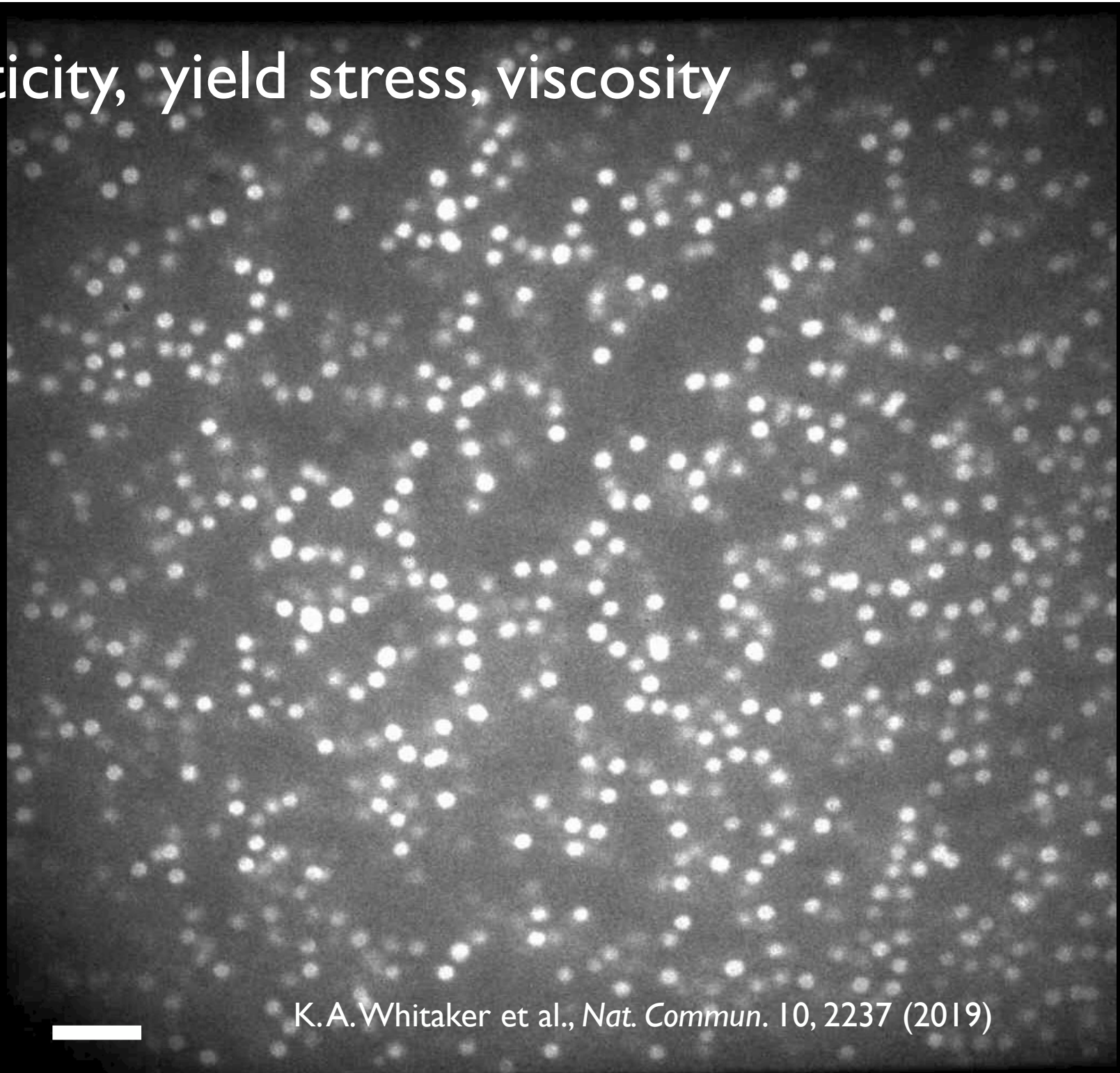

K. A. Whitaker et al., *Nat. Commun.* 10, 2237 (2019)

Cauchy-Born cluster model of gel modulus

Zaccone, A.; Wu, H.; Del Gado, E. *Phys. Rev. Lett.* 2009, 103, 208301.
Kobelev, V. & Schweizer, K. S. *J. Chem. Phys.* 2005, 123, 164902–164913
Ramakrishnan, S.; Chen, Y.-L.; Schweizer, K. S.; Zukoski, C. F. *Phys. Rev. E* 2004, 70, 40401.
K. A. Whitaker et al., Nat. Commun. 10, 2237 (2019).

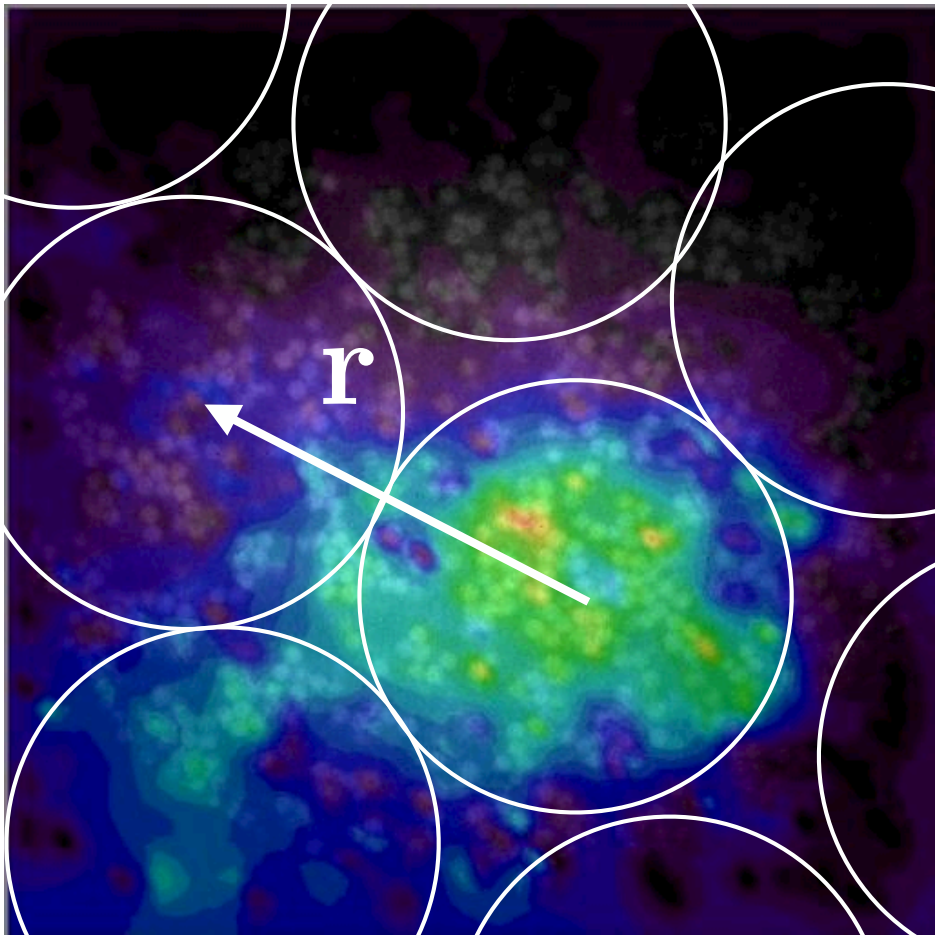

$$G' = 4n_e \kappa \langle r^2 \rangle$$

number density of elastic bonds × *bond stiffness* × *weighted cluster separation*

$$\langle r^2 \rangle = (1/3) \int (r_x r_y + r_y r_z + r_x r_z) P(\mathbf{r}) d\mathbf{r}$$

Distribution of cluster-cluster contacts $P(\mathbf{r})$

Depletion gels

Depletion gels

Ramakrishnan, S.; Chen, Y.-L.; Schweizer, K. S.; Zukoski, C. F. *Phys. Rev. E* 2004, 70, 40401.

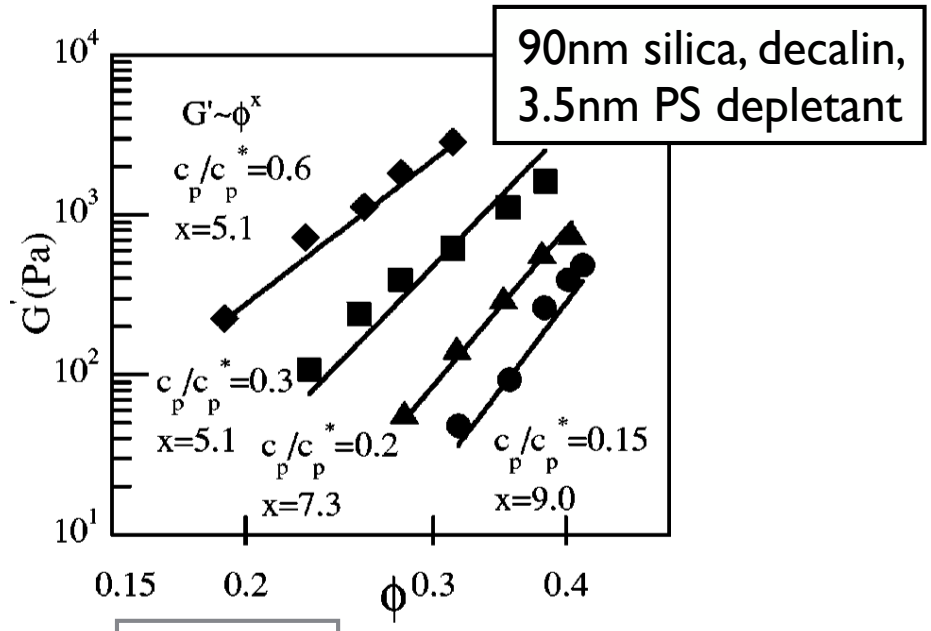

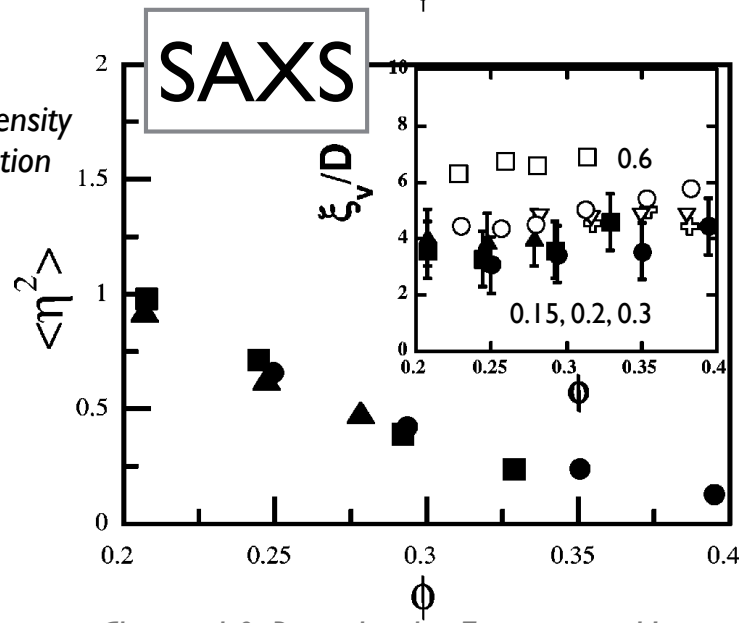

max density fluctuation

Cluster size *(solid symbols)*

weak function of volume fraction, polymer conc.

$$S(q) = \frac{S(0)}{(1 + q^2\xi_v^2)^2}$$

Bond level elasticity from PRISM theory

$$G'_{\mathrm{MCT}} = \frac{2.32\phi}{8a}\frac{kT}{r_{\mathrm{loc}}^2}$$

works, but only when shifted by number of clusters

$$G' \approx G'_{\mathrm{MCT}}/N_{pc}$$

$$N_{pc} = 8\phi_{pc}(\xi/2a)^3 = \phi_{pc}(\xi/a)^3$$

$$G' = \left(\frac{2.32}{8}\frac{a^2}{\xi^2}\right)\phi_c\frac{kT}{\xi r_{\mathrm{loc}}^2}$$

$$\kappa_0 = \frac{kT}{r_{\mathrm{loc}}^2}$$

$$G' = \left(\frac{2.32}{8}\frac{a^2}{\xi^2}\right)\phi_c\frac{\kappa_0}{\xi}$$

Clusters – micromechanical units of depletion gels

M. H. Lee and E. M. Furst, *Phys. Rev. E* 77, 041408 (2008).

Local strain propagation generated by forced probe

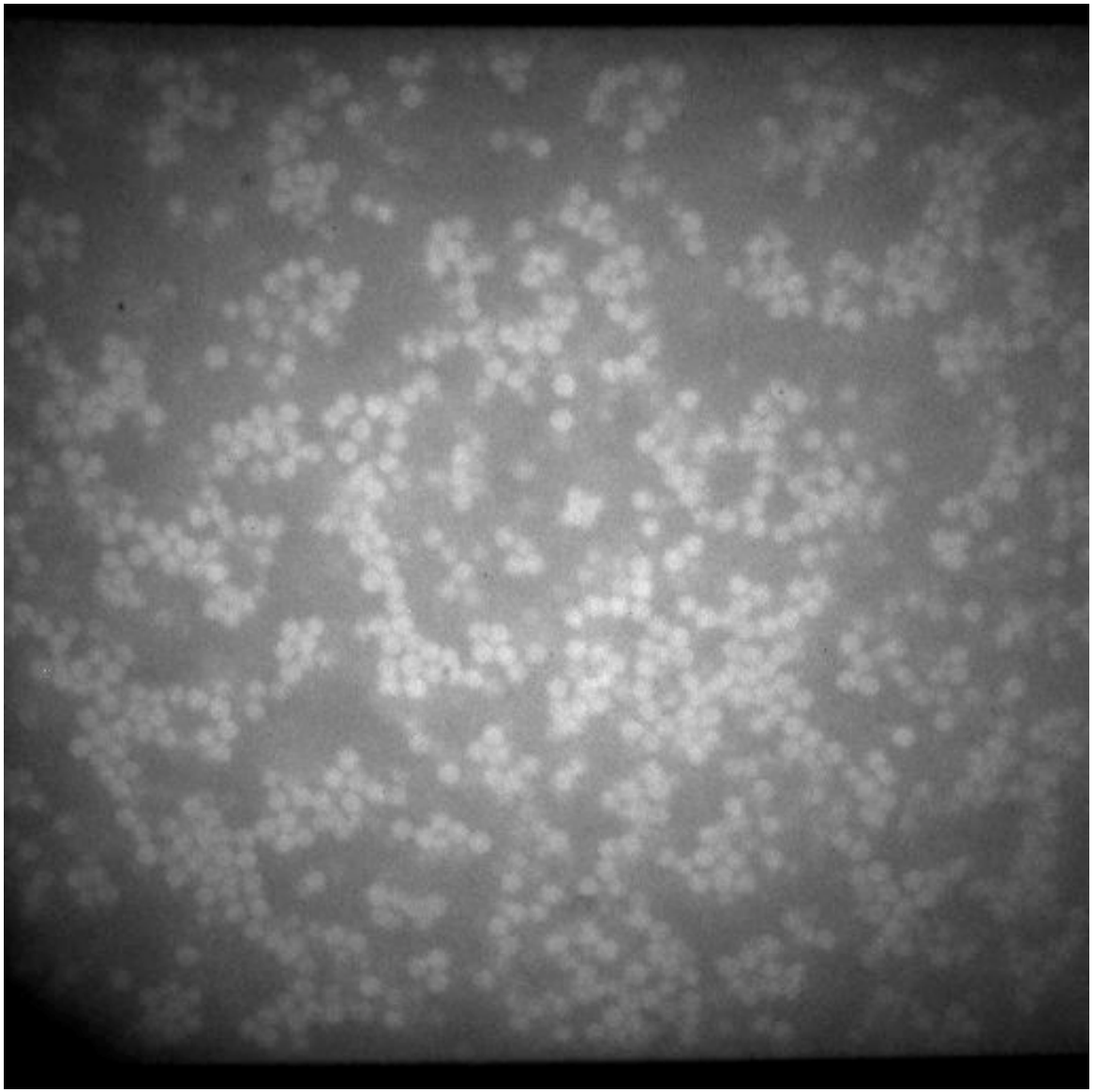

1.5µm PMMA, Φ= 0.22, Cp= 10mg/ml

Overlay of strain field with confocal image
1.5µm PMMA, Φ= 0.22, Cp= 10mg/ml

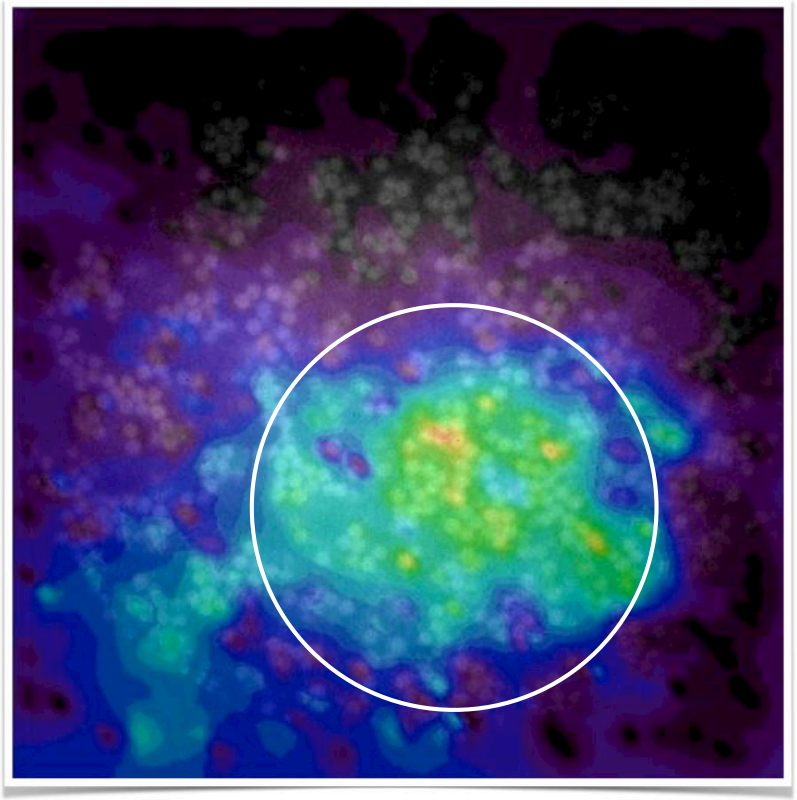

Clusters are rigid, units of strain propagation

M. H. Lee and E. M. Furst, Phys. Rev. E 77, 041408 (2008)

Displacement field from probe

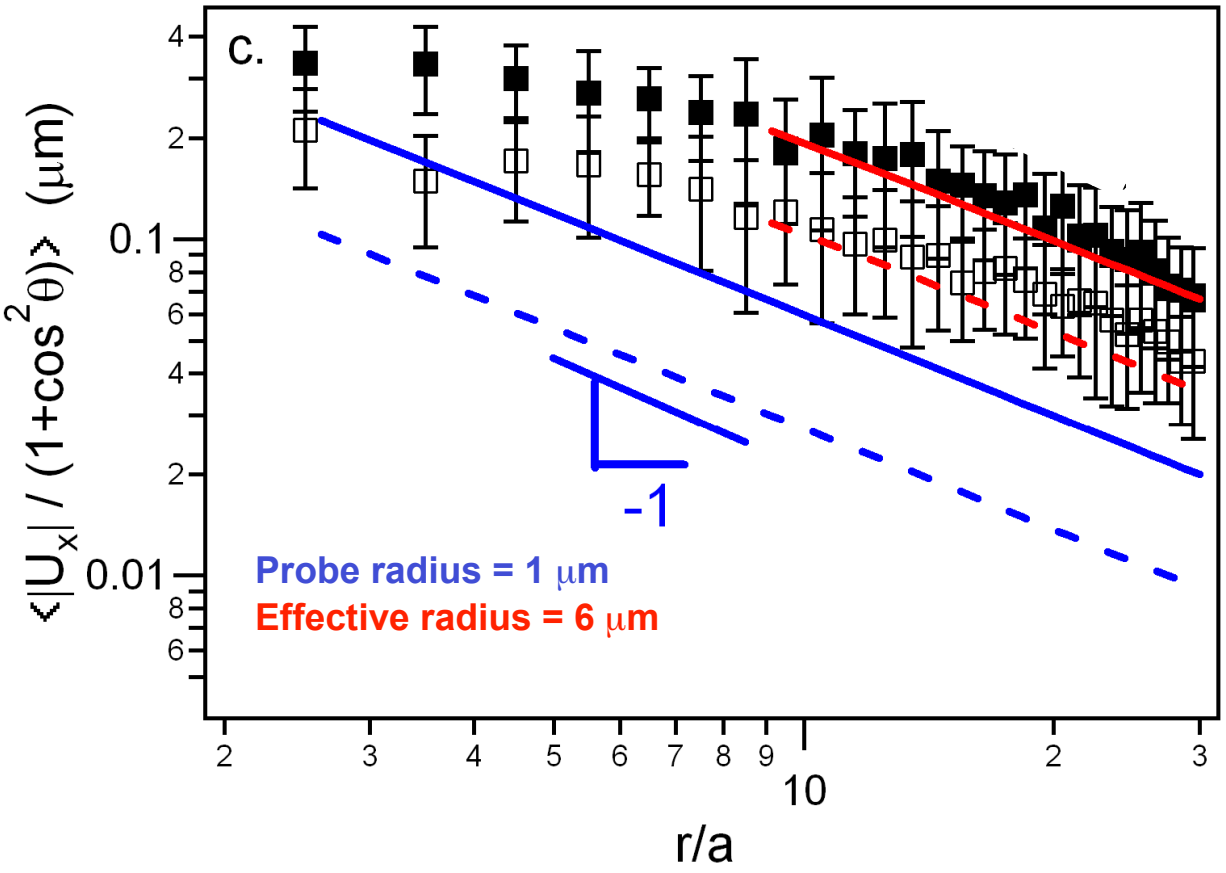

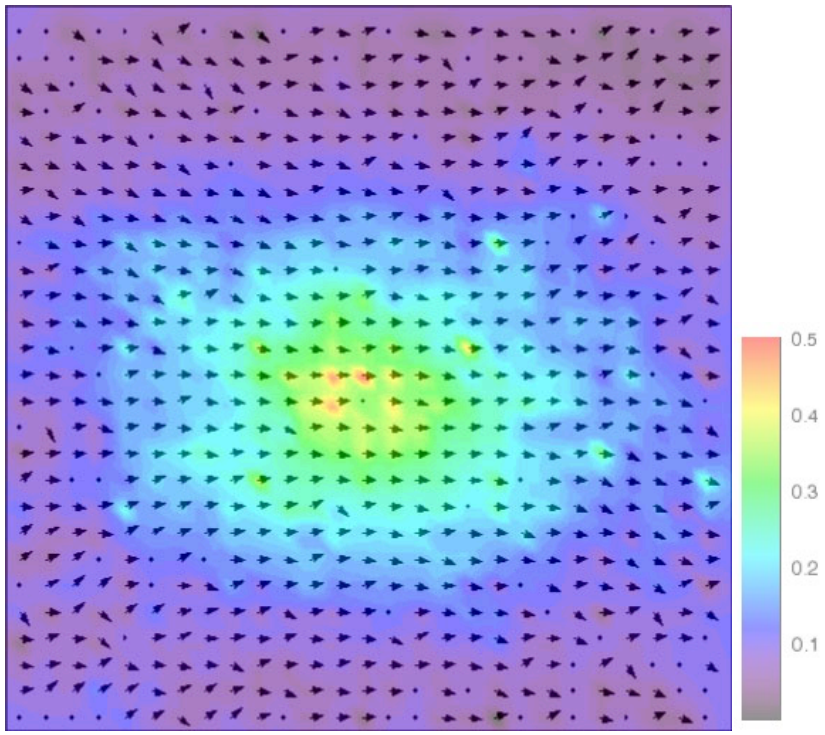

Laser amplitudes
open symbols: 0.55μm
closed symbols: 1.09μm

C_p = 10mg/ml 1.5μm PMMA, Φ= 0.22

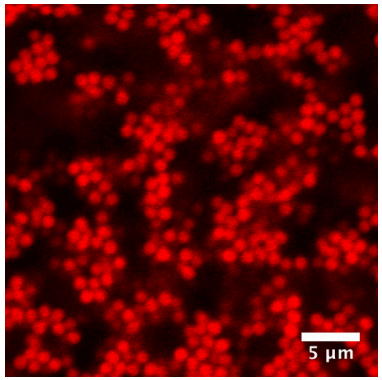

Depletion attraction

Asakura, S. & Oosawa, F. J Chem Phys 22, 1255–1256 (1954).
Vrij, A. Pure Appl. Chem. 48, 471–483 (1976).

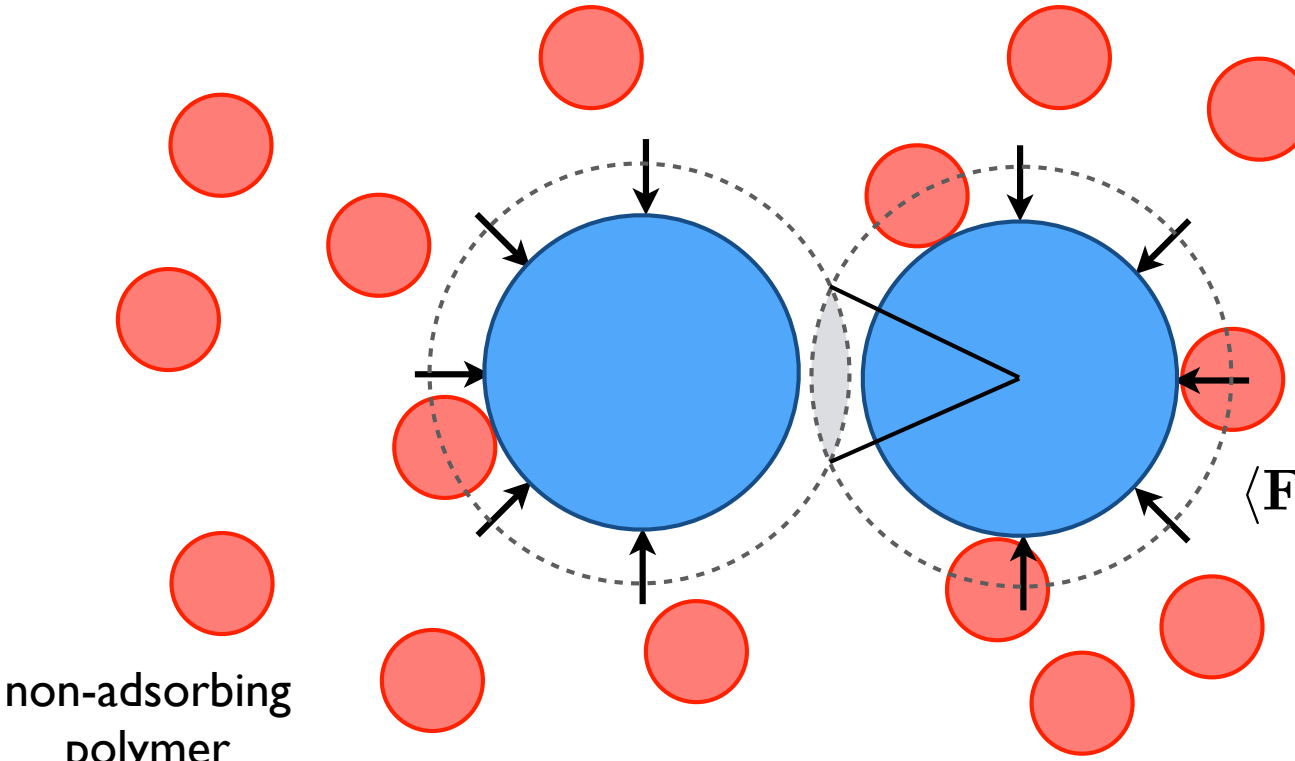

non-adsorbing polymer

osmotic pressure

$$\Pi$$

$$\langle \mathbf{F} \rangle_i = -nkT \oint \mathbf{n}_i g dS_i$$

Asakura-Oosawa interaction potential

$$\frac{U(r)}{k_B T} \approx \phi_p \left\{ 1 - \frac{3r}{4R(1+R_g/R)} + \frac{1}{2}\left[\frac{r}{2R(1+R_g/R)}\right]^3 \right\}$$

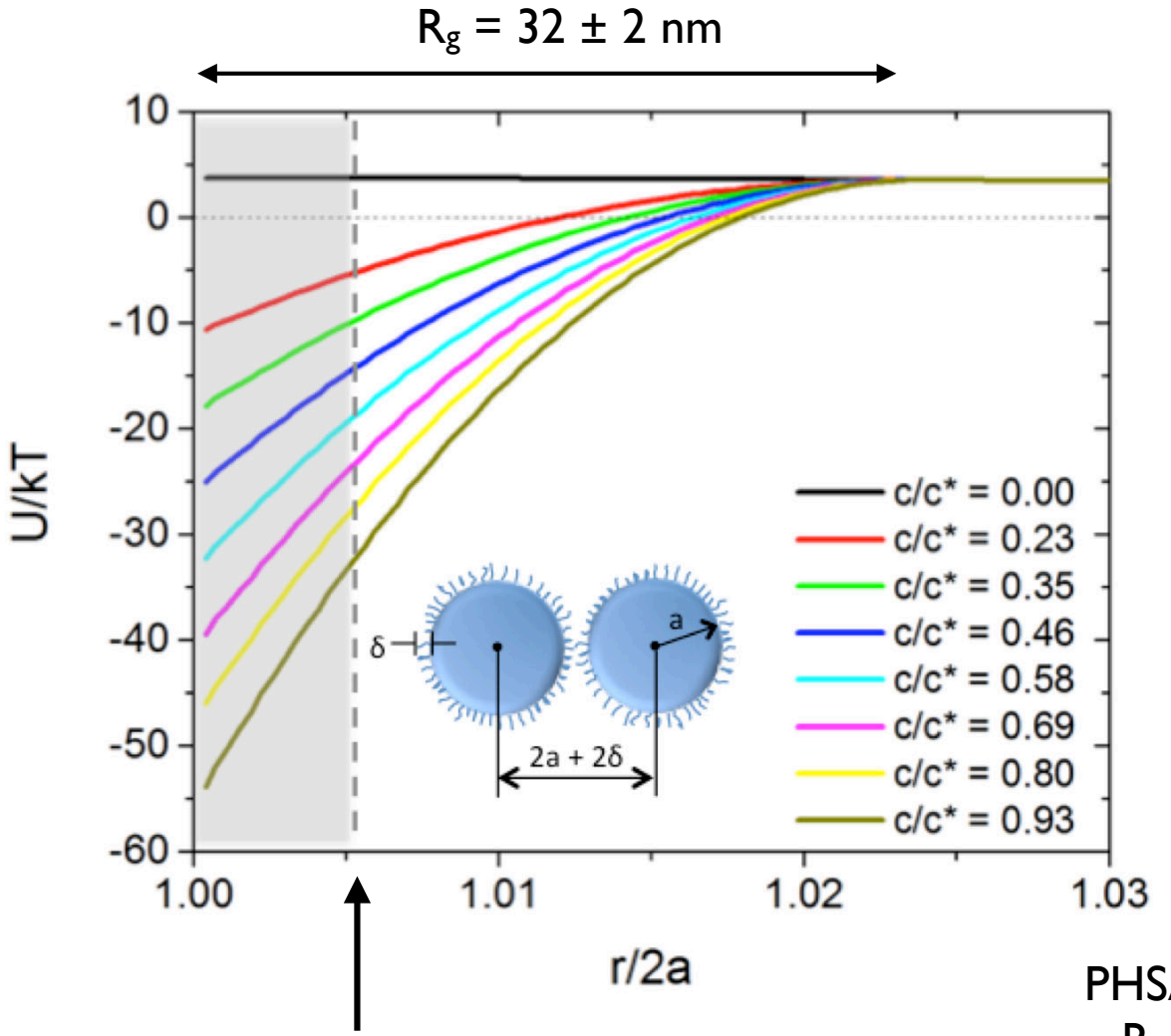

PHSA brush cutoff, 7nm

PHSA-PMMA 2a = 2.7 μm, R_g = 32 ± 2 nm, Steric brush length δ = 7 nm

Depletion "bonds" between colloids

Whitaker, K.A. & Furst, E. M. *J. Rheology* 60, 517–529 (2016).
Swan, J.W., Shindel, M. & Furst, E. M. *Phys. Rev. Lett.* 109, 198302 (2012).

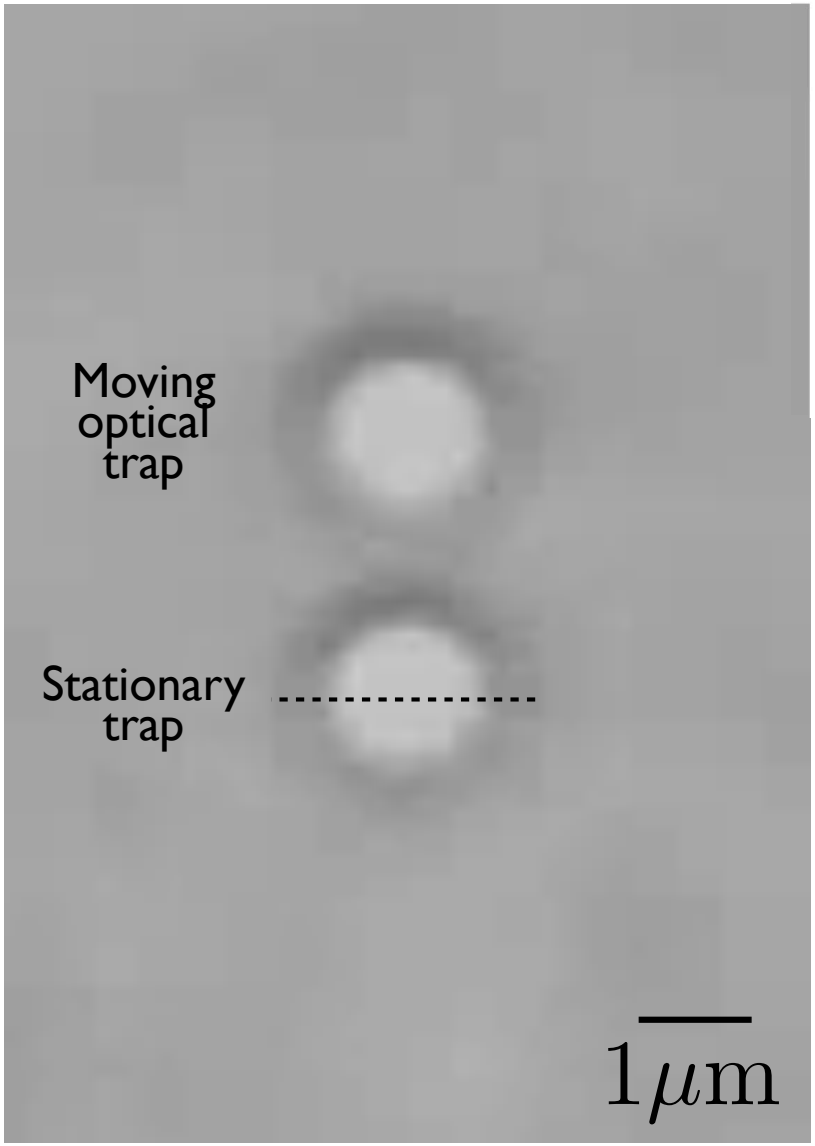

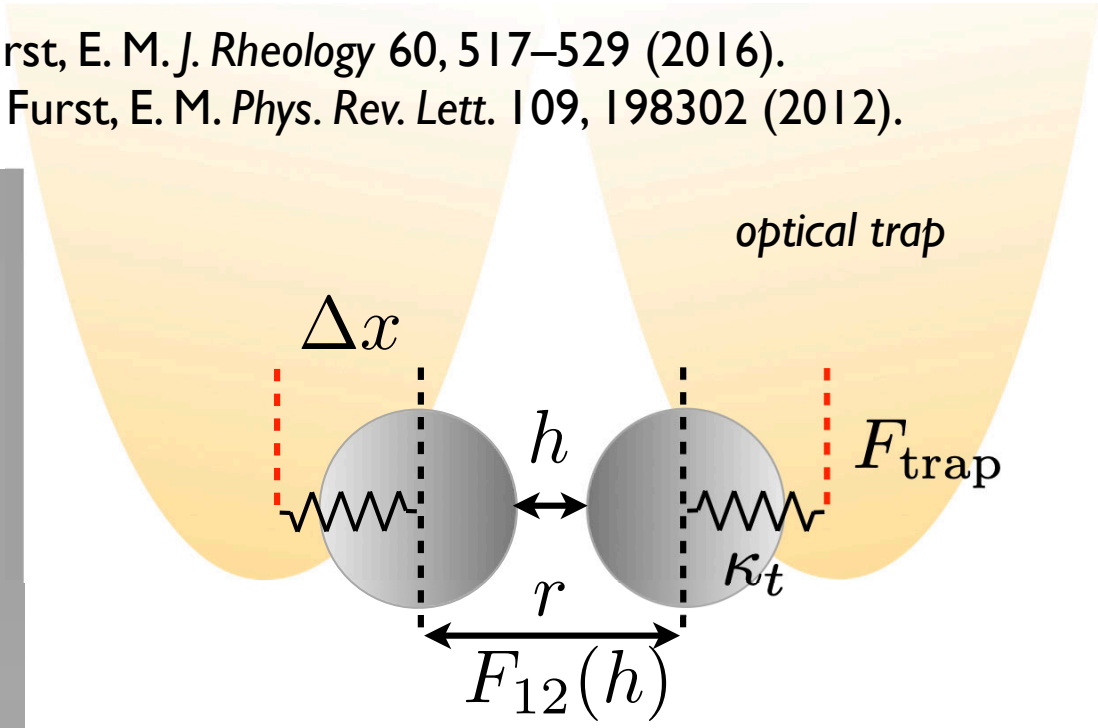

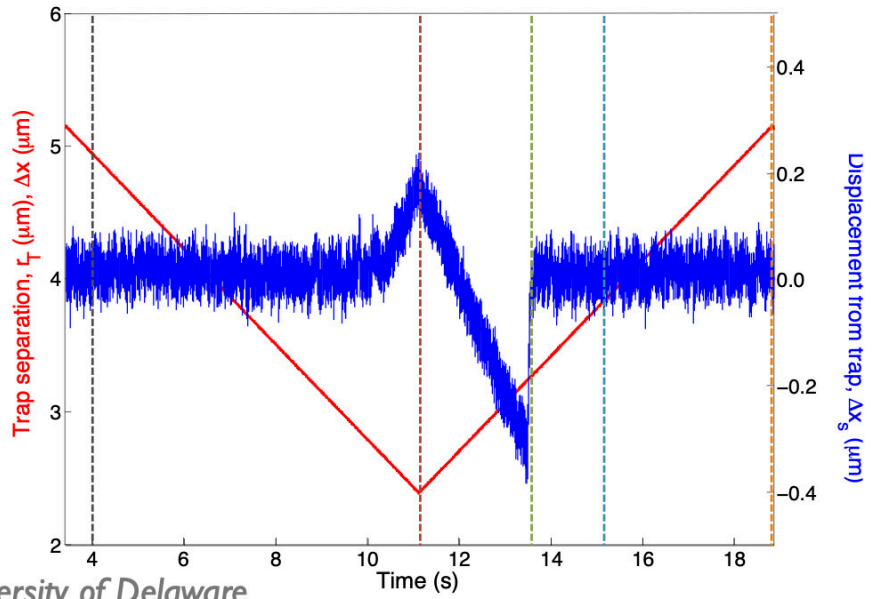

Thermal bond rigidity for depletion attraction

Whitaker, K.A. & Furst, E. M. *J. Rheology* 60, 517–529 (2016).

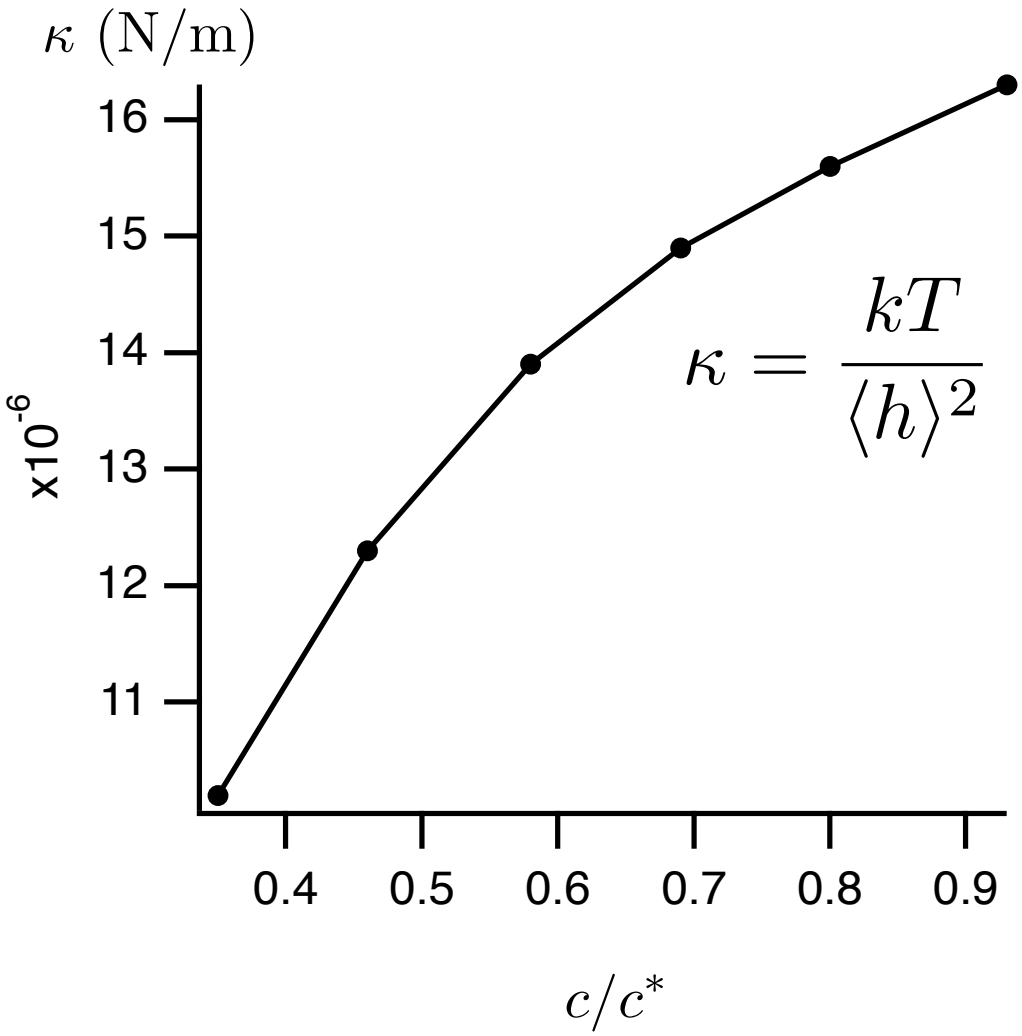

PHSA-PMMA in cyclohexane/cyclohexyl bromide

Depletion gel modulus

PHSA-PMMA in cyclohexane/cyclohexyl bromide ($\phi = 0.2$)

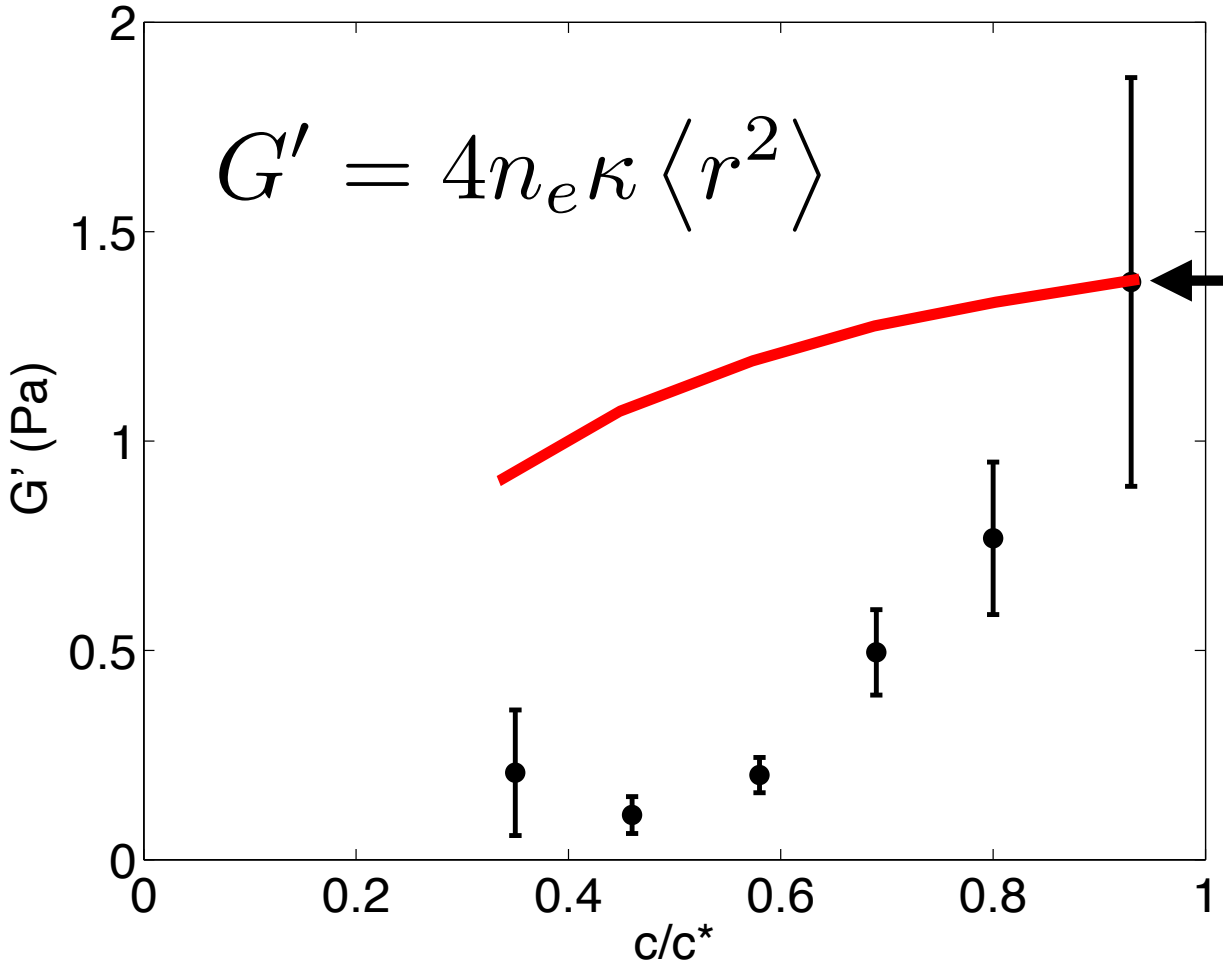

Calculated with measured bond rigidity

Whitaker, K. A. & Furst, E. M. *J. Rheology* 60, 517–529 (2016).
Swan, J. W., Shindel, M. & Furst, E. M. *Phys. Rev. Lett.* 109, 198302 (2012).

Experiments and simulations

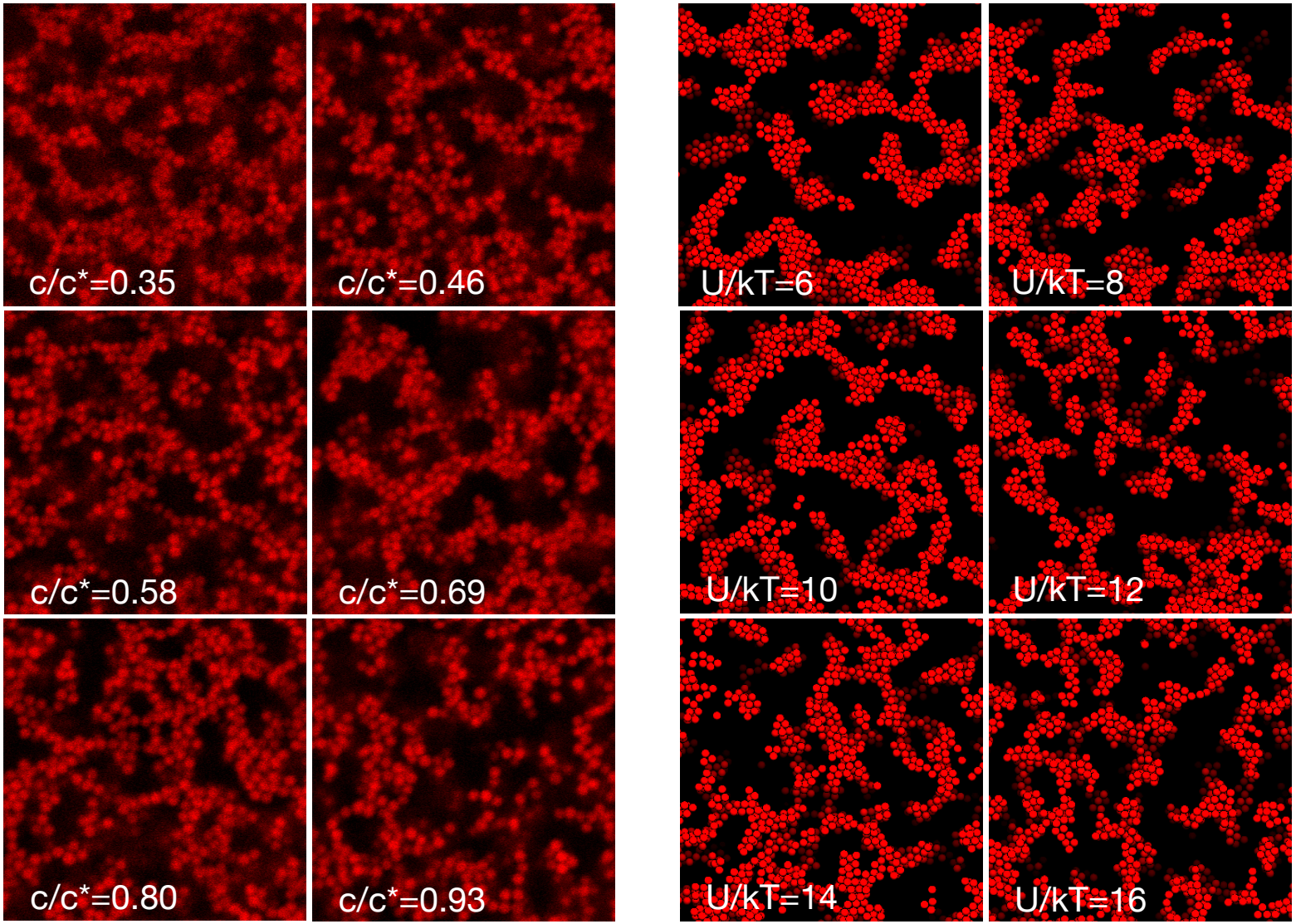

Whitaker, Hsiao, Solomon & Furst

Swan and Varga

Simulations: Fiore, Usabiaga, Donev, & Swan, *J. Chem. Phys.* 146, 124116 (2017).

Gel structure correlation length

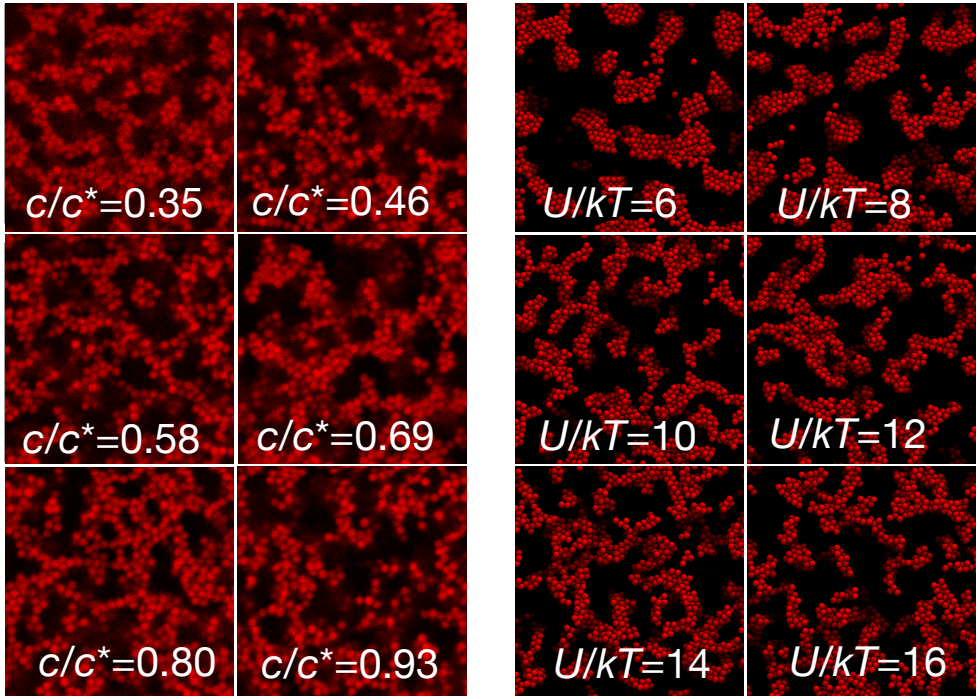

Number density fluctuation

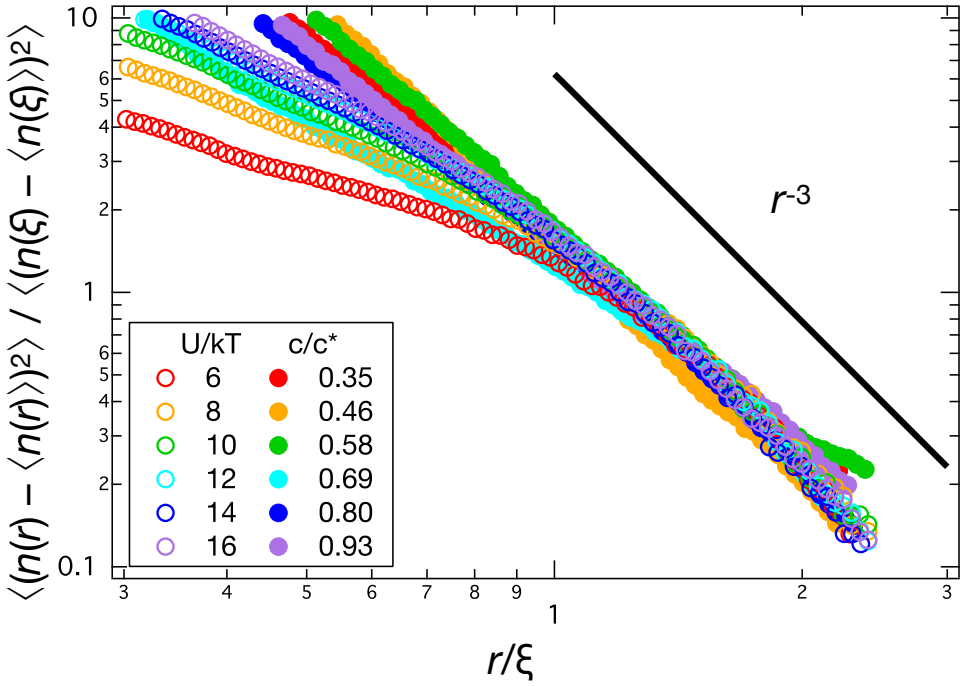

Also observed by Ramakrishnan et al. for 90nm silica in decalin, PS depletant

Ramakrishnan, S.; Chen, Y.-L.; Schweizer, K. S.; Zukoski, C. F. *Phys. Rev. E* 2004, 70, 40401.

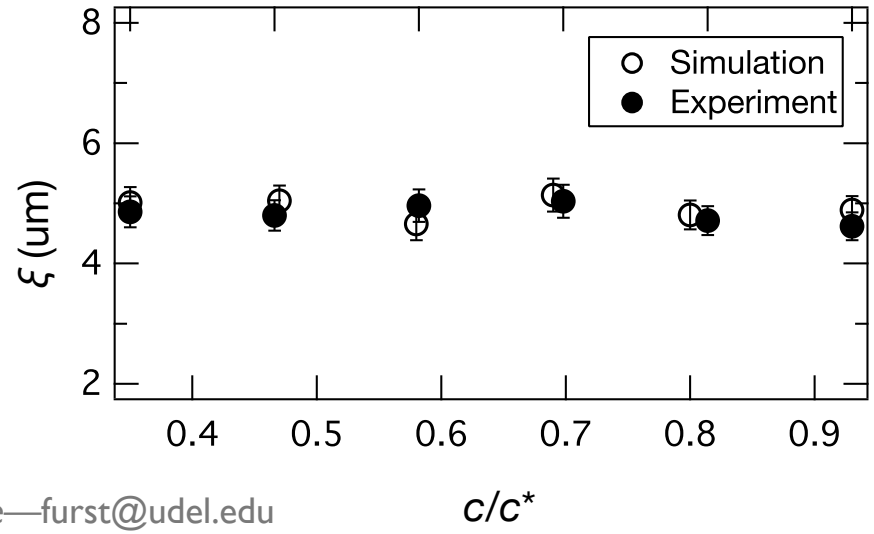

Simulations quantitatively describe structure and rheology

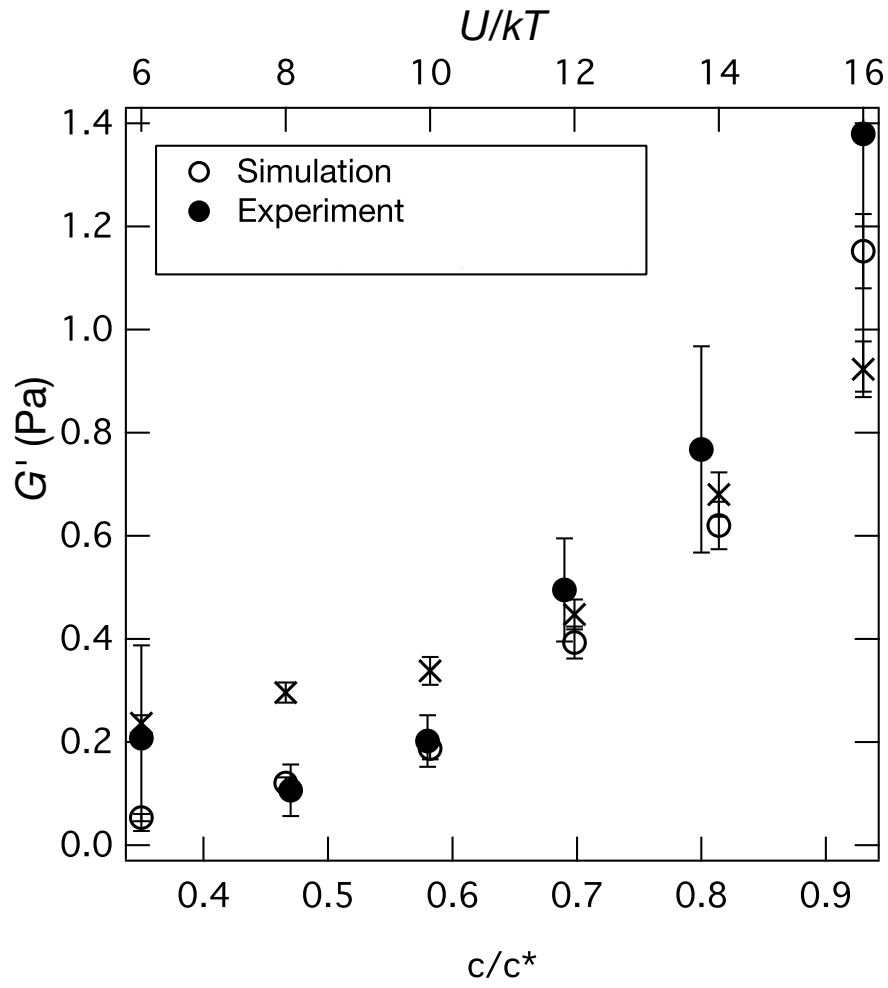

Cauchy-Born cluster model of gel modulus

Zaccone, A.; Wu, H.; Del Gado, E. *Phys. Rev. Lett.* 2009, 103, 208301.
Kobelev, V. & Schweizer, K. S. *J. Chem. Phys.* 2005, 123, 164902–164913
Ramakrishnan, S.; Chen, Y.-L.; Schweizer, K. S.; Zukoski, C. F. *Phys. Rev. E* 2004, 70, 40401.

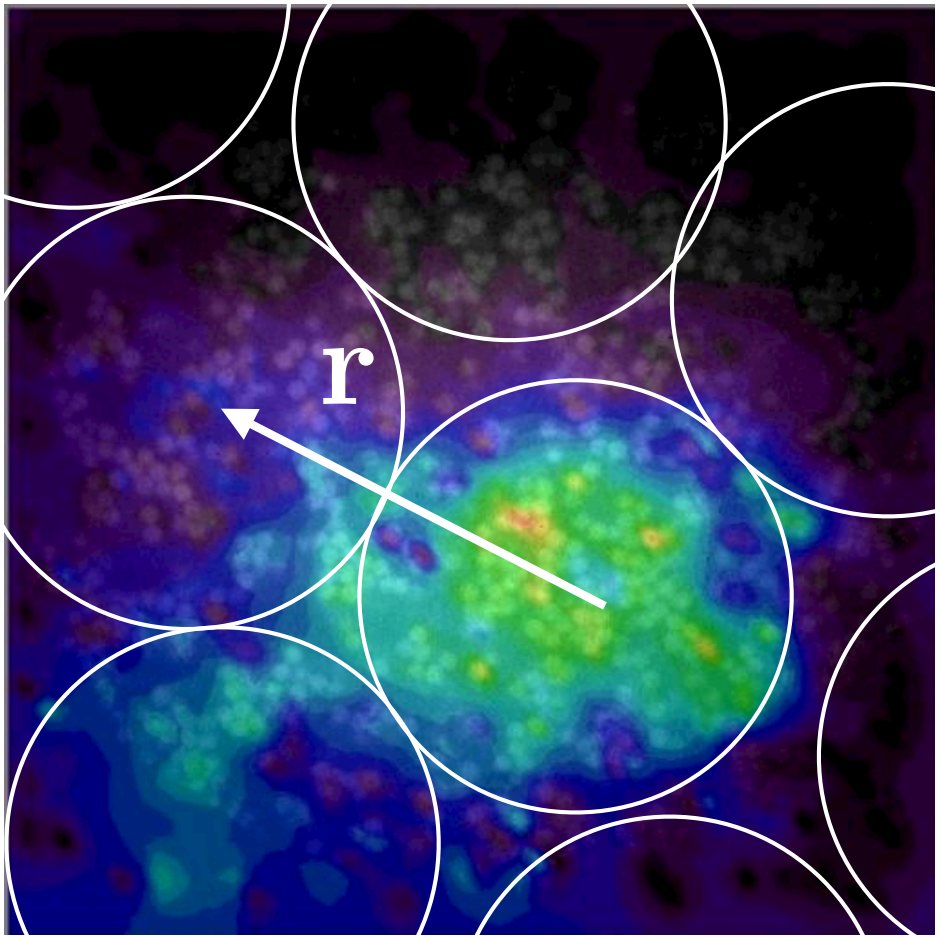

$$G' = 4 n_e \kappa \left\langle r^2 \right\rangle$$

number density of elastic bonds × *bond stiffness* × *weighted cluster separation*

$$\left\langle r^2 \right\rangle = (1/3) \int (r_x r_y + r_y r_z + r_x r_z) P(\mathbf{r}) d\mathbf{r}$$

Distribution of cluster-cluster contacts $P(\mathbf{r})$

$$n_e = \frac{1}{2} n_c z_c$$

number density of clusters × *average cluster contacts*

Where are clusters? How do they connect?

Confocal microscopy

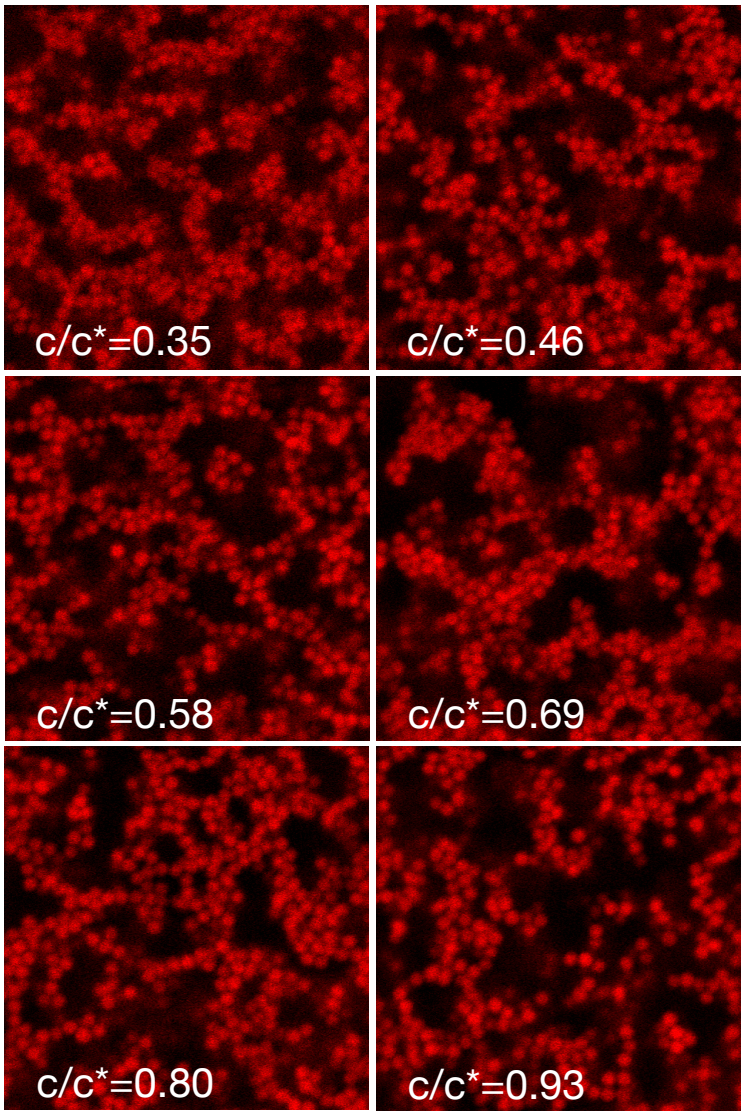

Whitaker, Hsiao, Solomon & Furst

Dynamic simulation

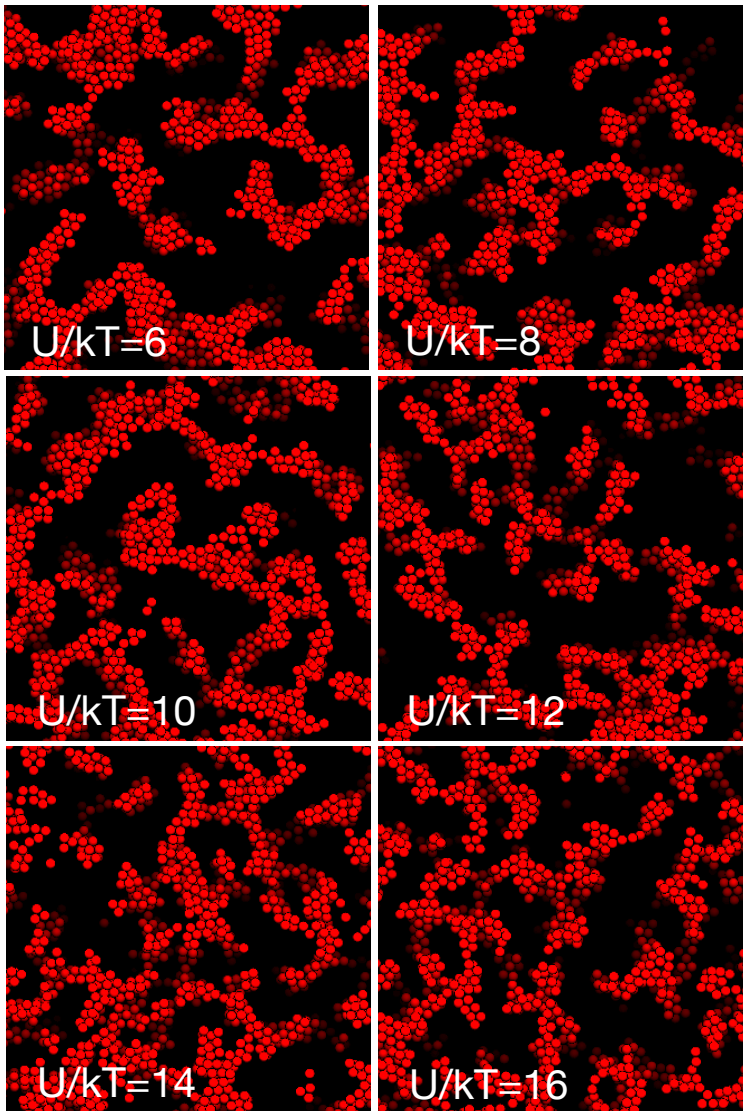

Swan and Varga

l-balanced graph partition

S. Zhong, J. Ghosh, Proceedings of the 2003 SIAM International Conference on Data Mining pp. 71–82 (2003).
J. P. Hespanha, An efficient Matlab algorithm for graph partitioning (2004).

K. A. Whitaker et al., *Nature Commun.* 10, 2237 (2019)

gel structure

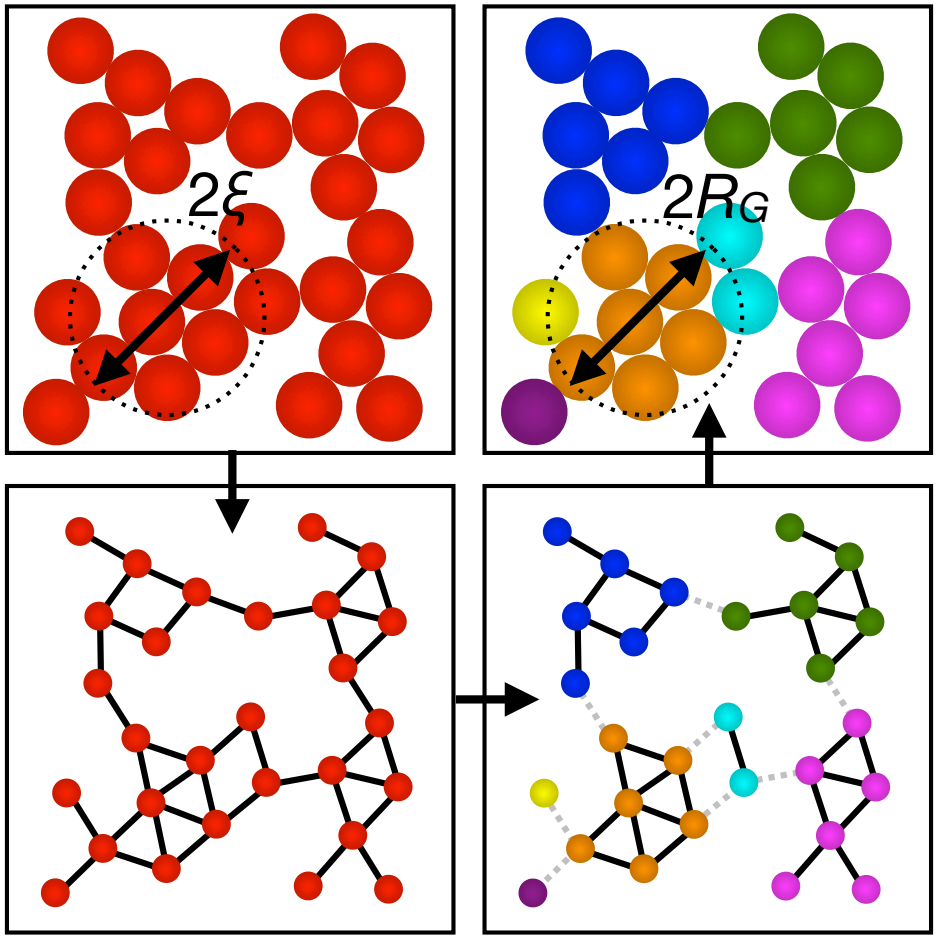

graph representation

l chosen to give $R_g = \xi$

cut fewest edges to create subgraphs of l vertices

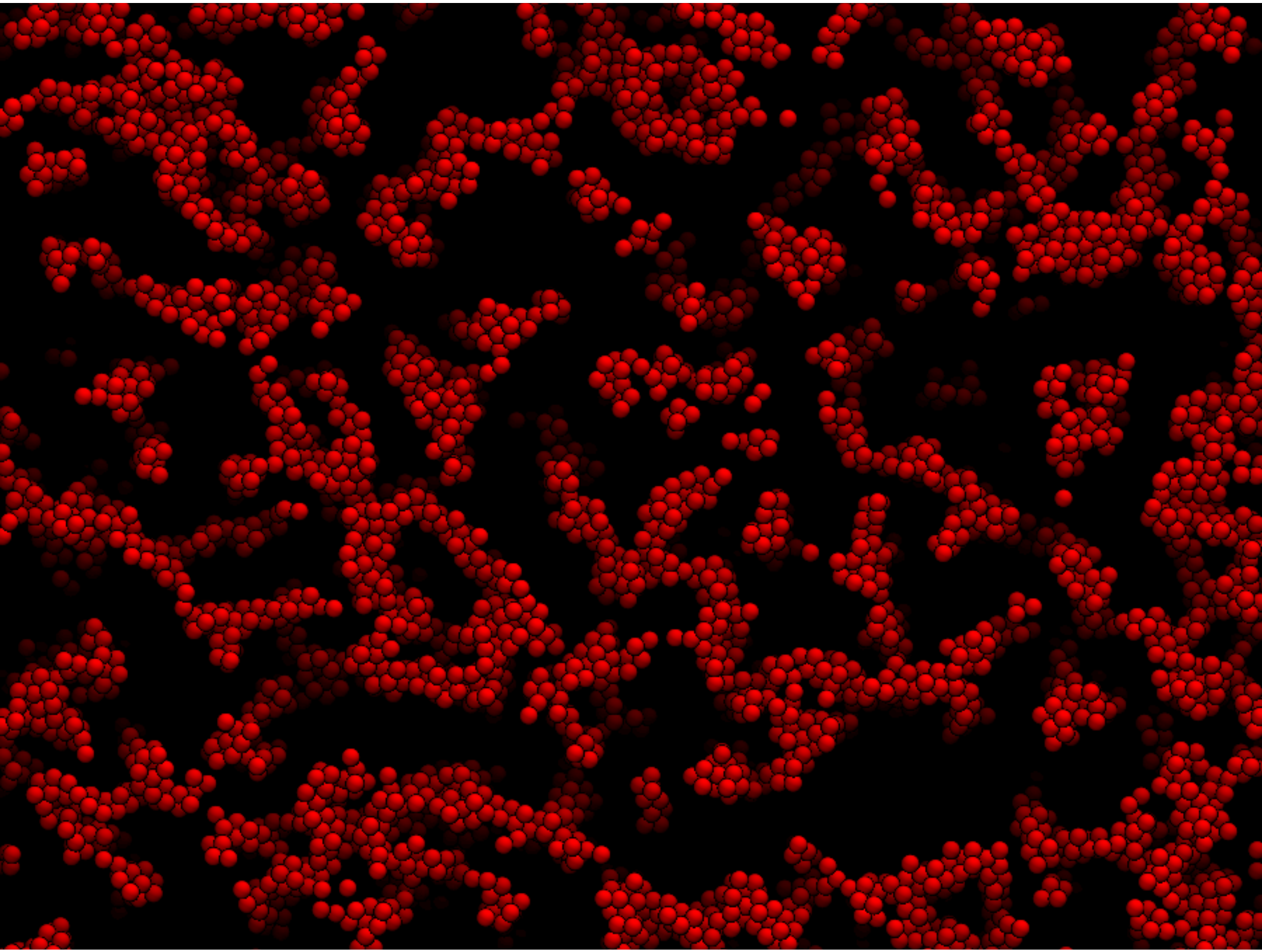

Cluster gel structure

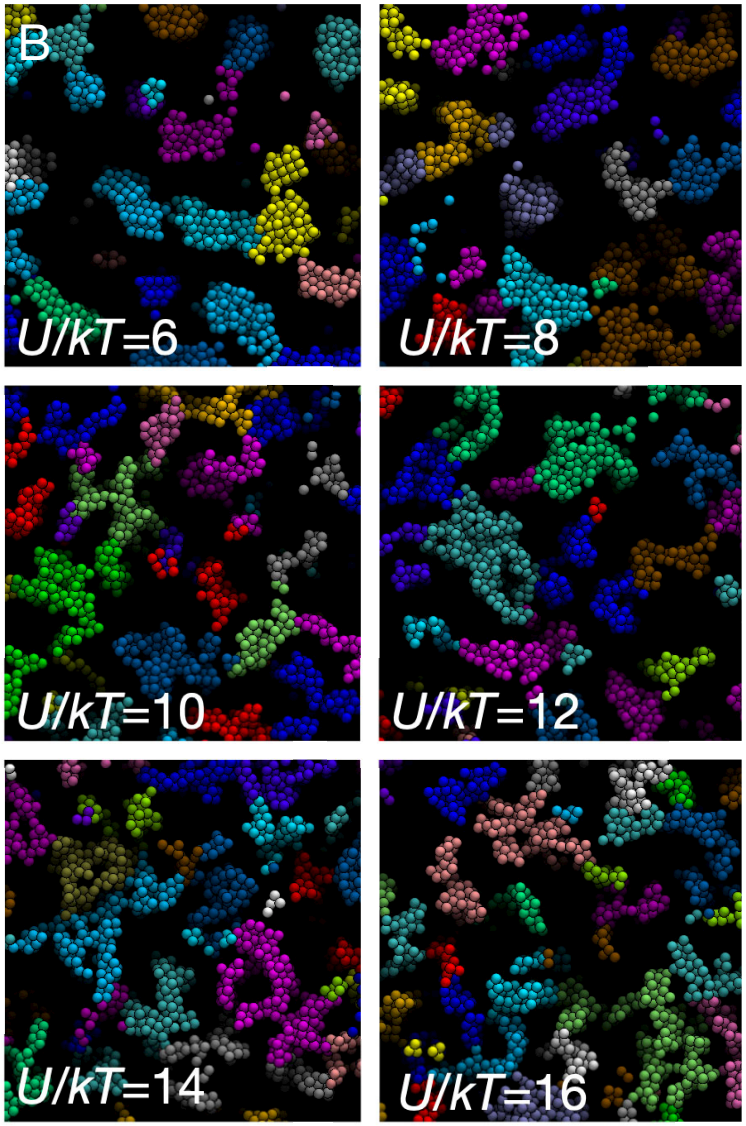

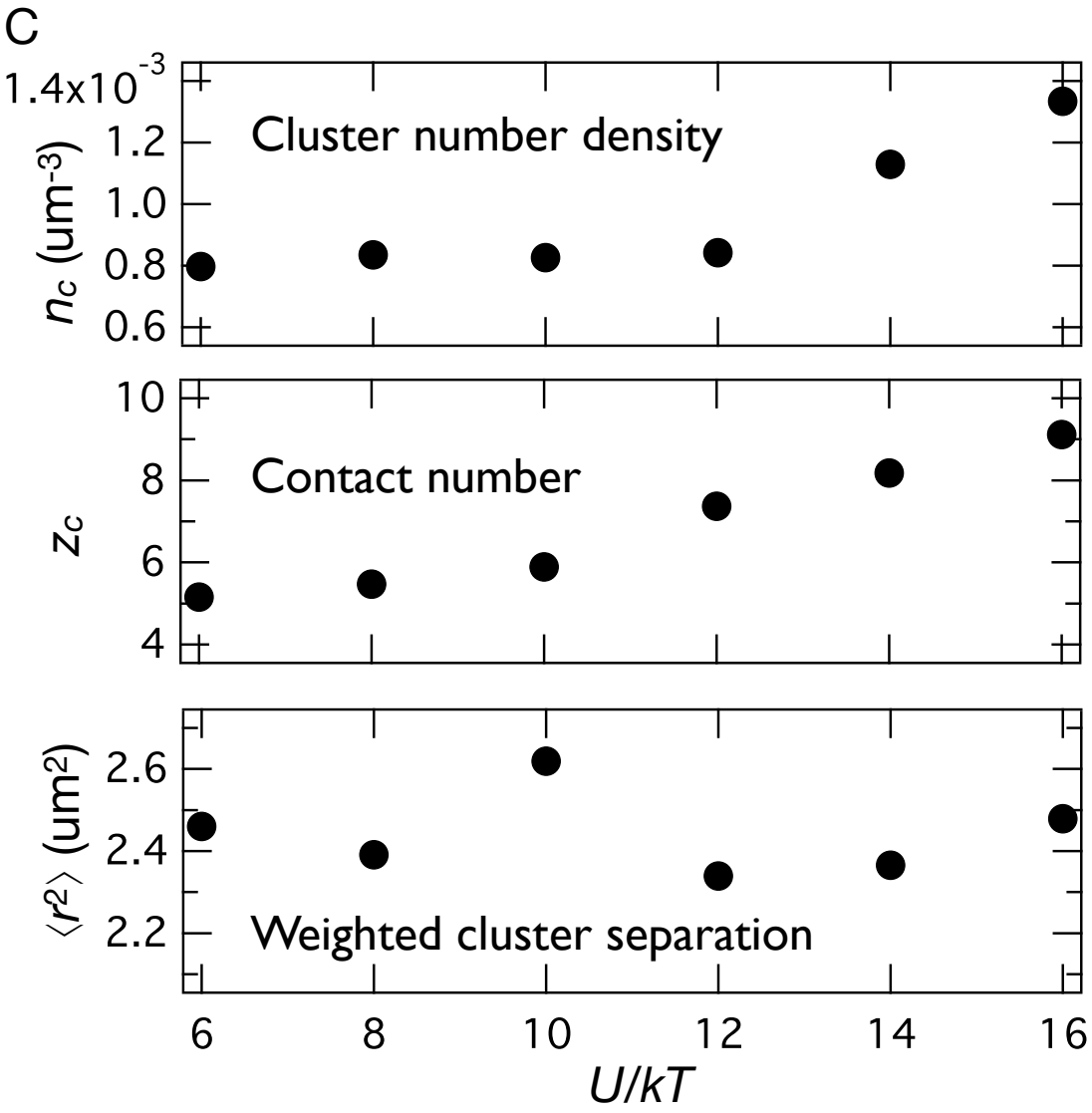

Cluster gel elasticity

$$G' = 2n_c z_c \kappa \left\langle r^2 \right\rangle$$

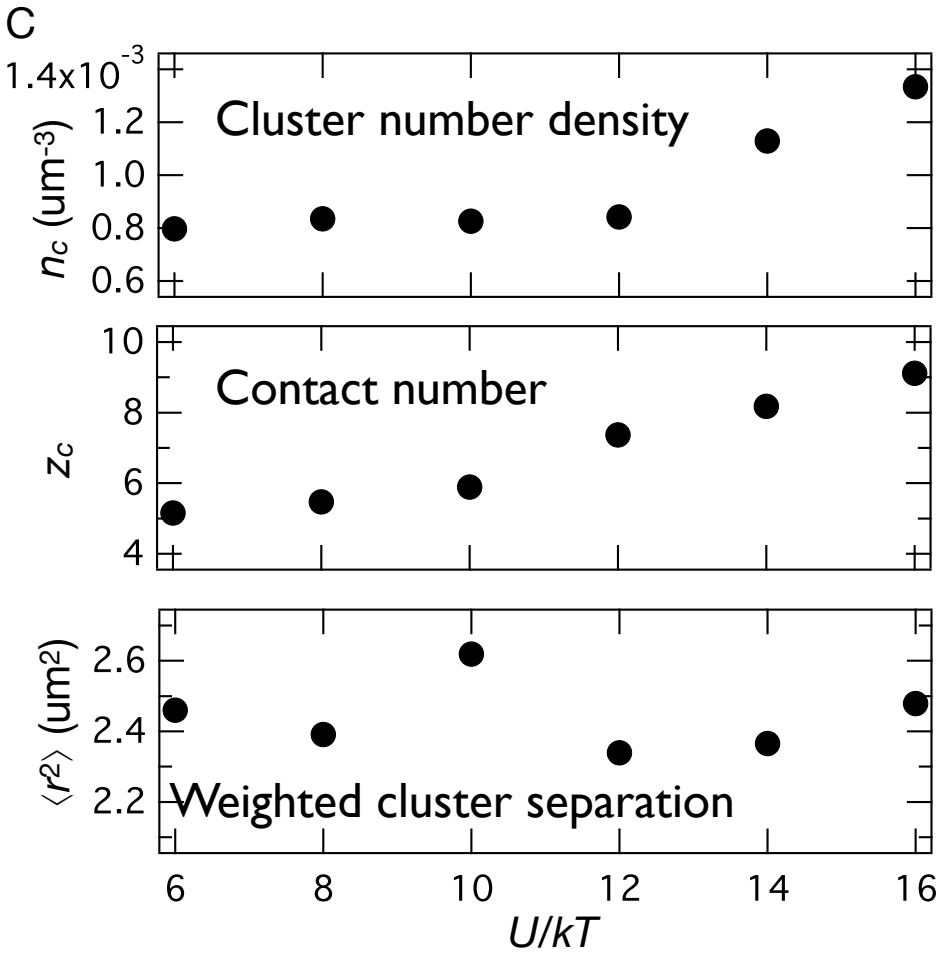

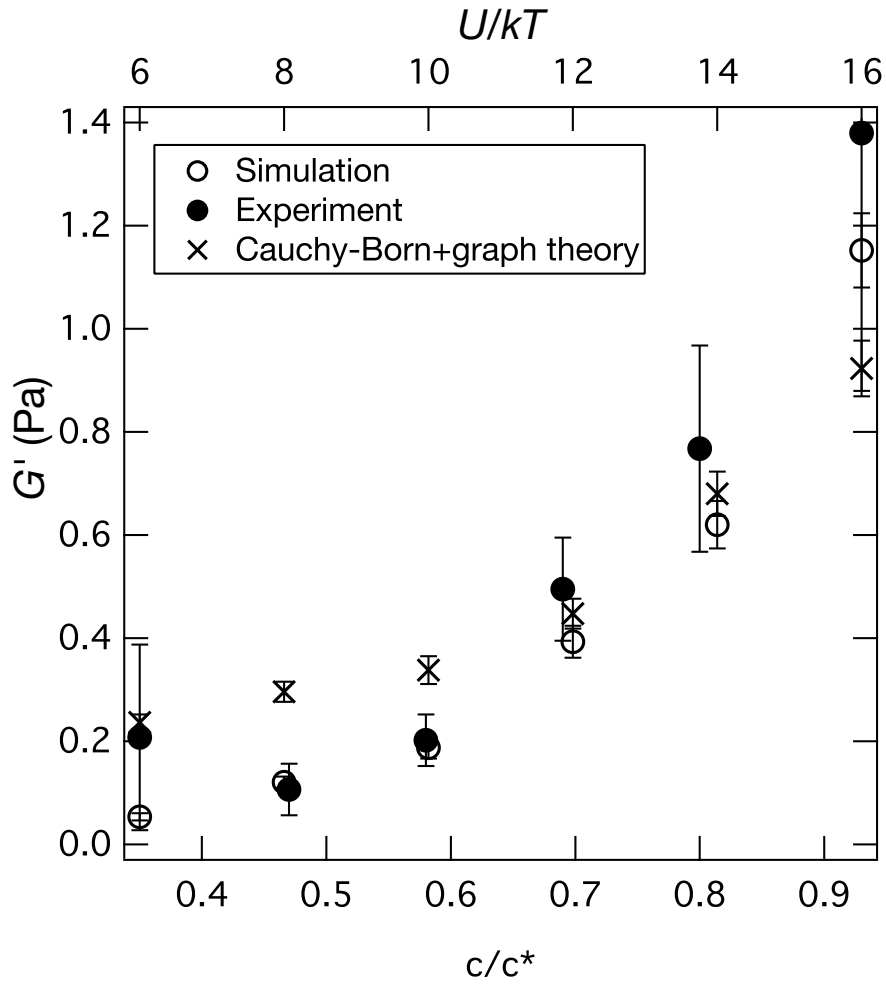

Some gel lines (of "passive" gels)

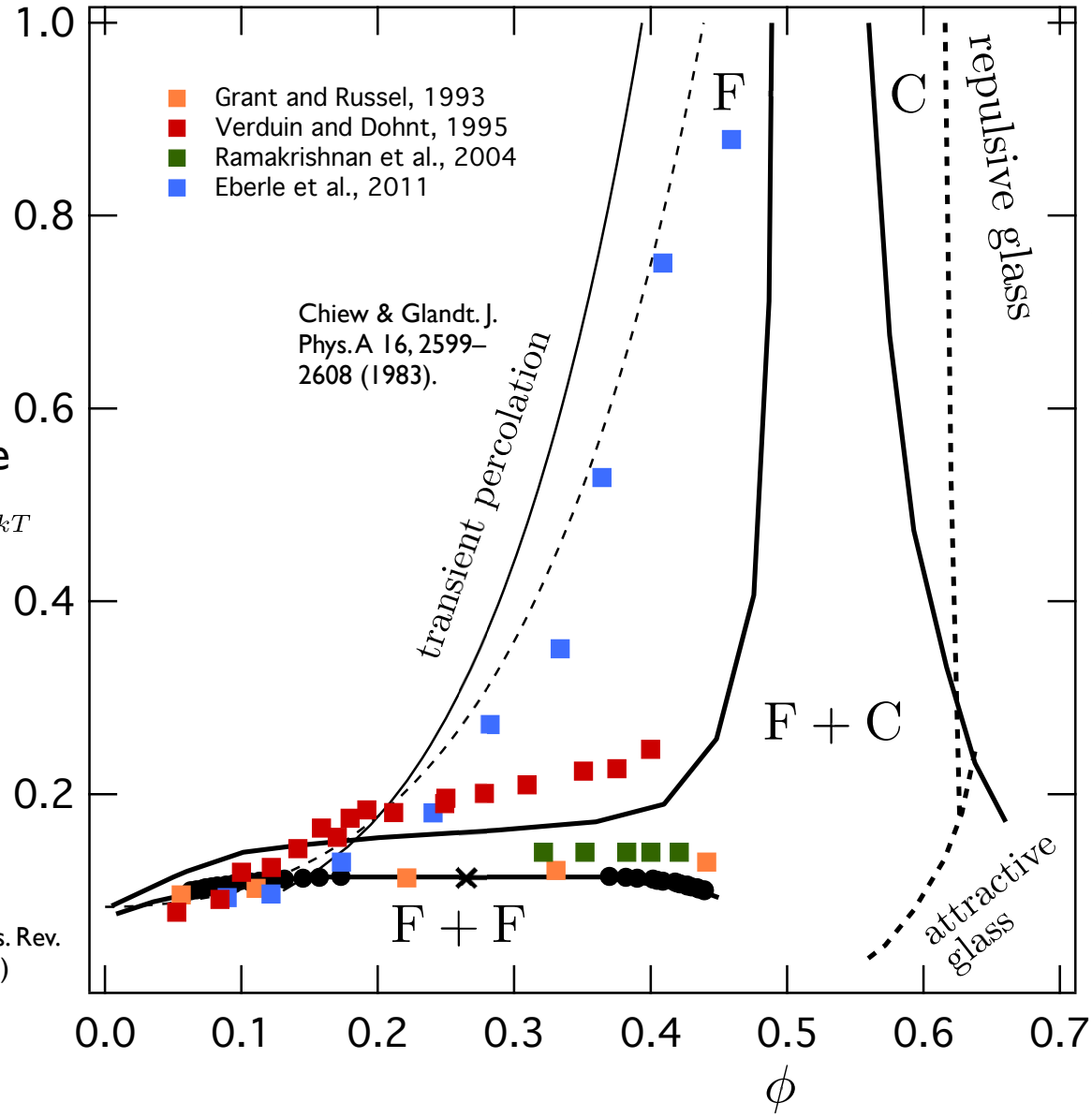

Pusey and van Megan, Phys. Rev. Lett. 59, 2083-2086 (1987)

Foffi et al. J Phys-Condens Mat 16, S3791-S3806 (2004)

Sciortino et al. Phys. Rev. Lett, 91, 268301 (2003)

Pham et al. Science 296, 104-106 (2002)

Baxter temperature

$$\tau_B = \left(\frac{2a+\Delta}{12\Delta}\right) e^{-\epsilon/kT}$$

Baxter, R. J., J.Chem. Phys. 49, 2770 (1968)

Miller and Frenkel. Phys. Rev. Lett. 90, 135702 (2003)

Density *in* cluster extends attractive glass line

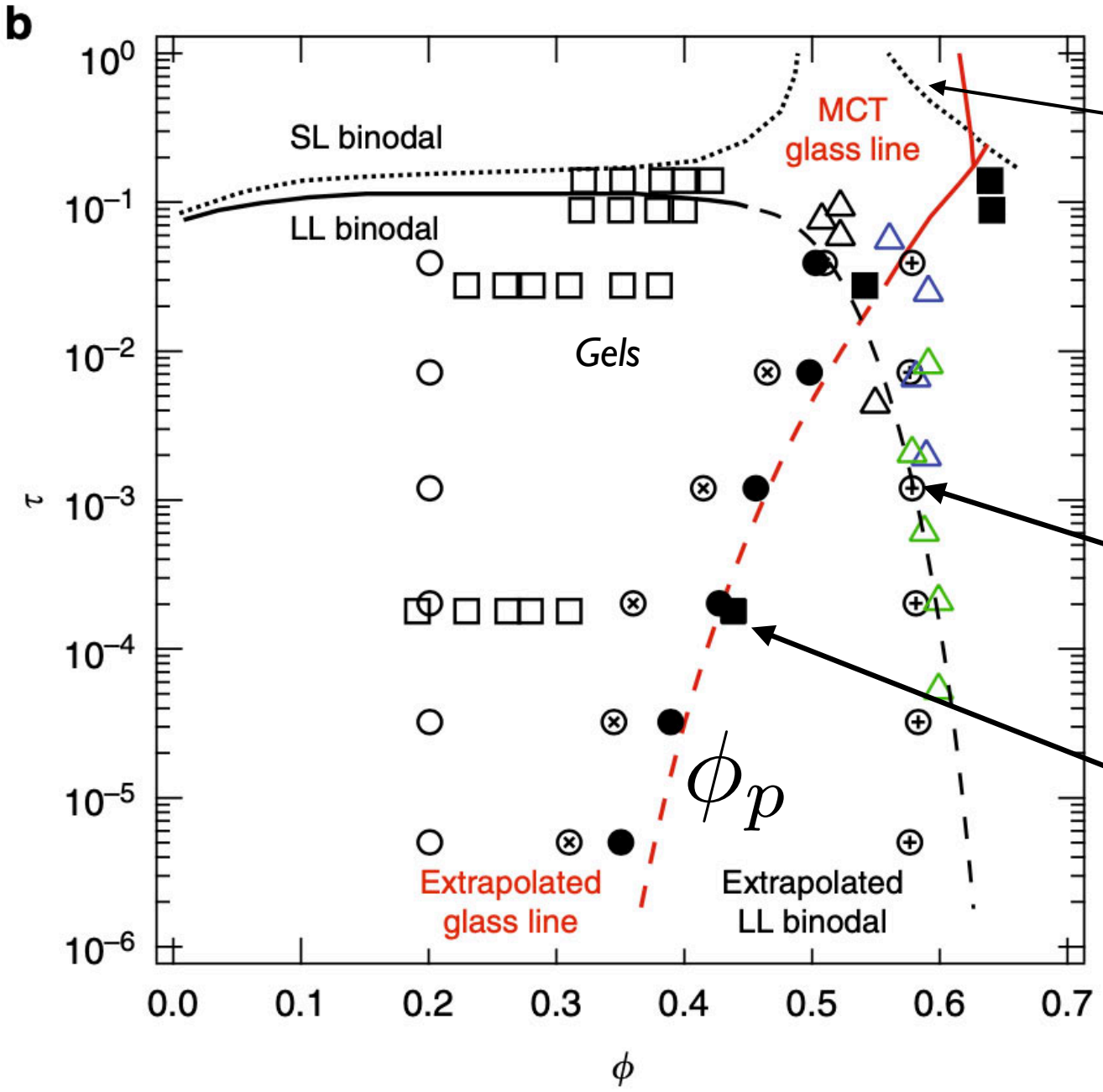

Equil. solid

P. J. Lu, E. Zaccarelli, F. Ciulla, A. B. Schofield, F. Sciortino, and D. A. Weitz, *Nature* 453, 499 (2008).

90nm silica, decalin, PS depletant

Ramakrishnan et al. *Phys. Rev. E* 2004, 70, 40401.

Acknowledgments

Francesco Bonacci
ESPCI

Xavier Chateau

Julie Goyon

Anaël Lemaître

Laboratoire Navier, Ecole des Ponts & Université Paris-Est

Silica particle gels

F. Bonacci et al., Nat. Mater. 19, 775–780 (2020).

1-2μm silica particles, ~38% volume fraction, high ionic strength (0.15M)

Elastic modulus "aging" over time

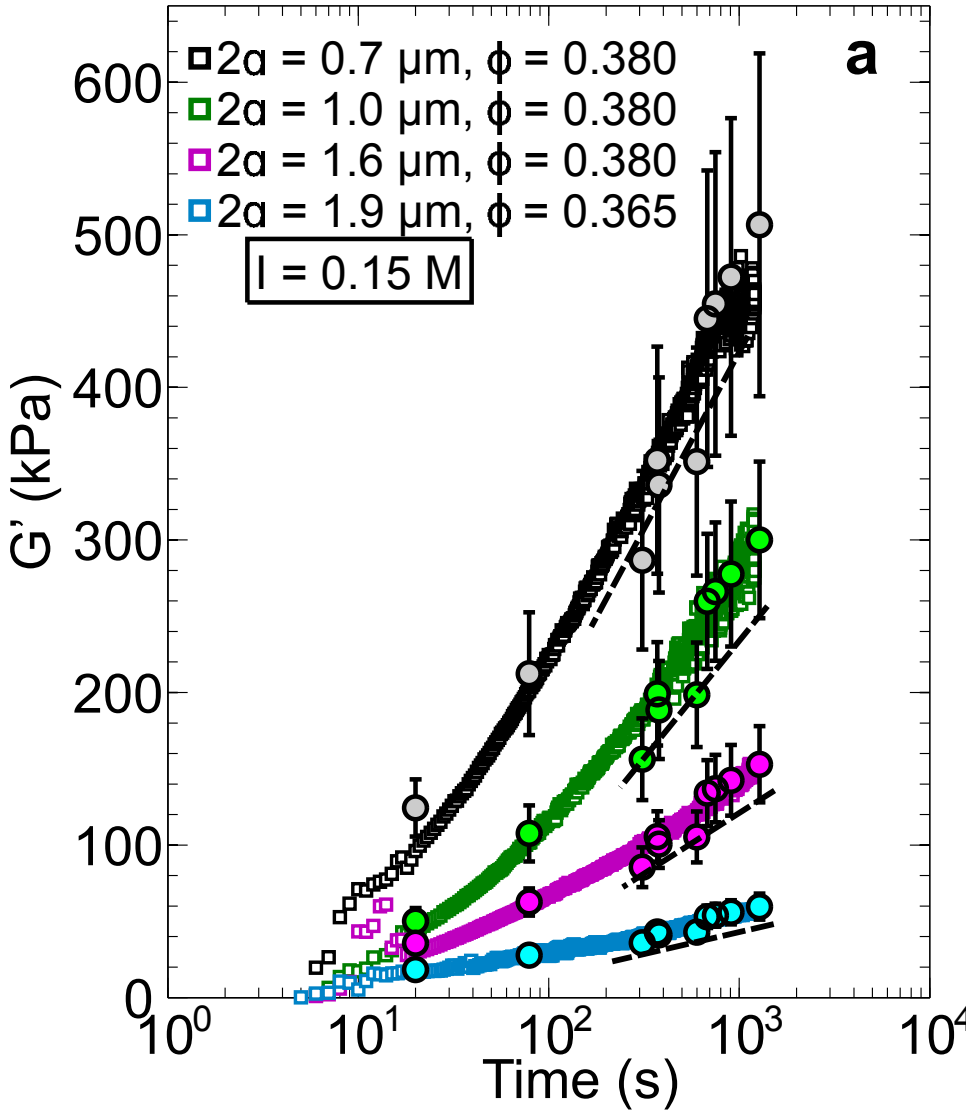

Aging of silica gels

F. Bonacci et al., *Nat. Mater.* 19, 775–780 (2020).
F. Bonacci, et al., *Phys. Rev. Lett.* 128, 018003 (2022).

1-2μm silica particles, ~38% volume fraction, high ionic strength (0.15M)

Elastic modulus

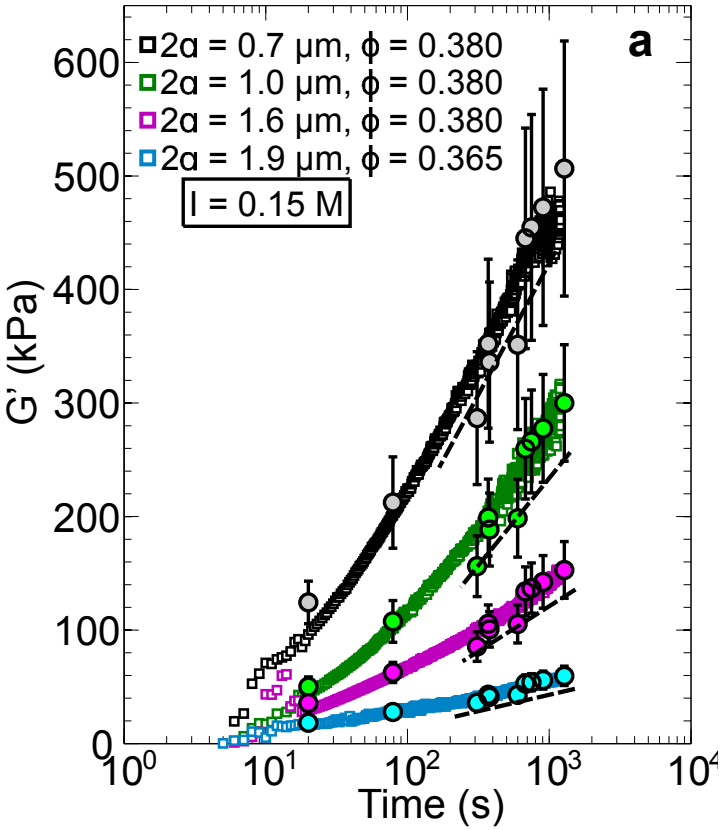

Confocal microscopy

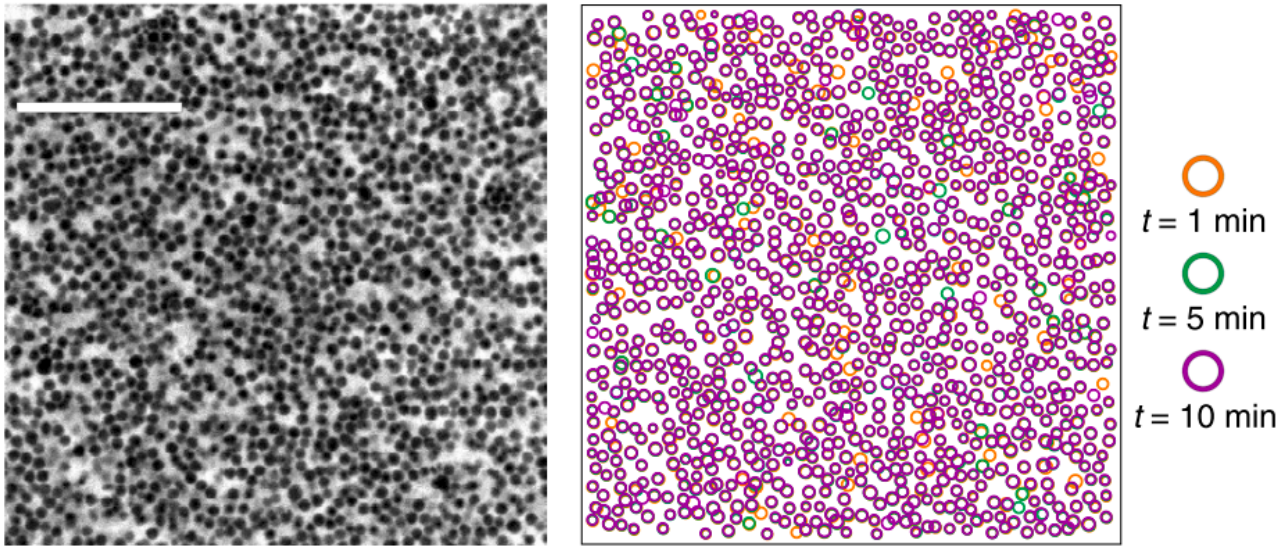

Despite modulus increase, no microstructure change!

Adhesion between particles

Johnson, Kendall and Roberts, *Proc. R. Soc. London, Ser. A* 324, 301 (1971).
Pantina and Furst, *Phys. Rev. Lett.* 94:138301 (2005).

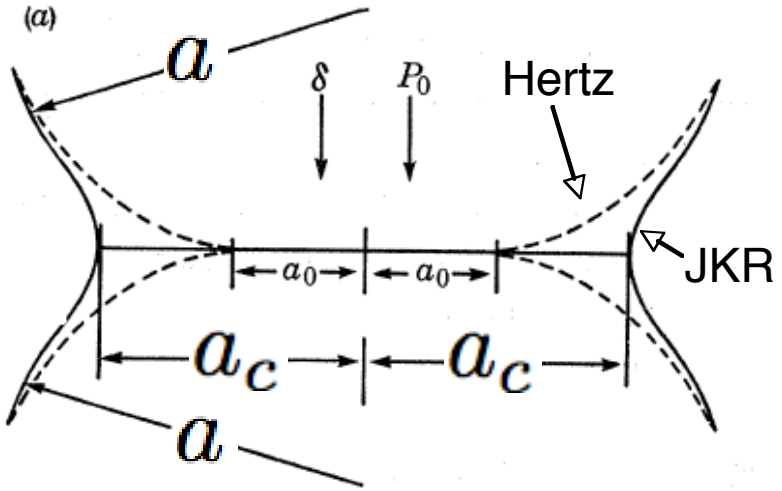

Single-bond rigidity:

$$\kappa_0 = \frac{3\pi E}{4a^3}\left(\frac{3\pi a^2 W_{SL}}{2K}\right)^{4/3}$$

Relates mechanics to adhesion energy (particle interfacial phenomena)

Bond rigidity in aging silica

F. Bonacci et al., *Nat. Mater.* 19, 775–780 (2020).
F. Bonacci, et al., *Phys. Rev. Lett.* 128, 018003 (2022).

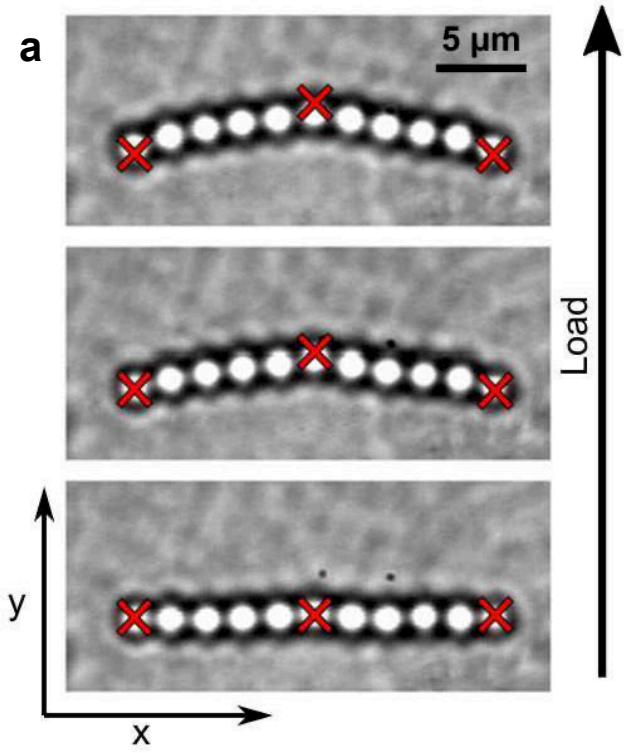

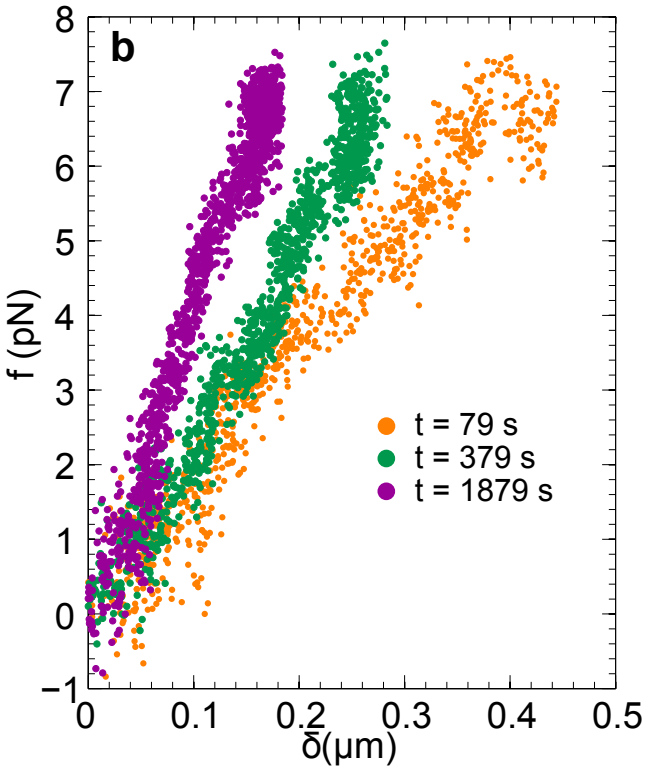

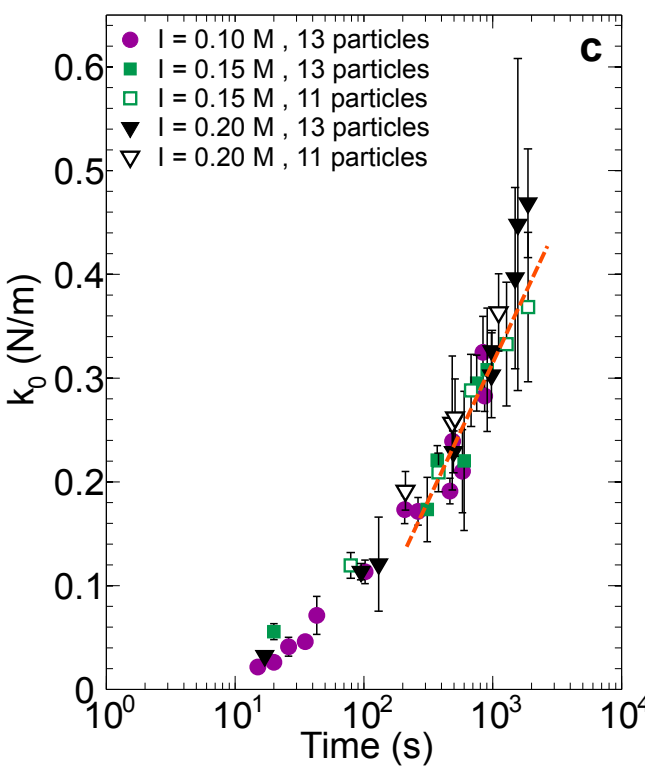

1-2μm silica particles, 38% volume fraction, high ionic strength (0.15M)

1 μm diameter Dynabead polystyrene latex with O(10)nm iron oxide

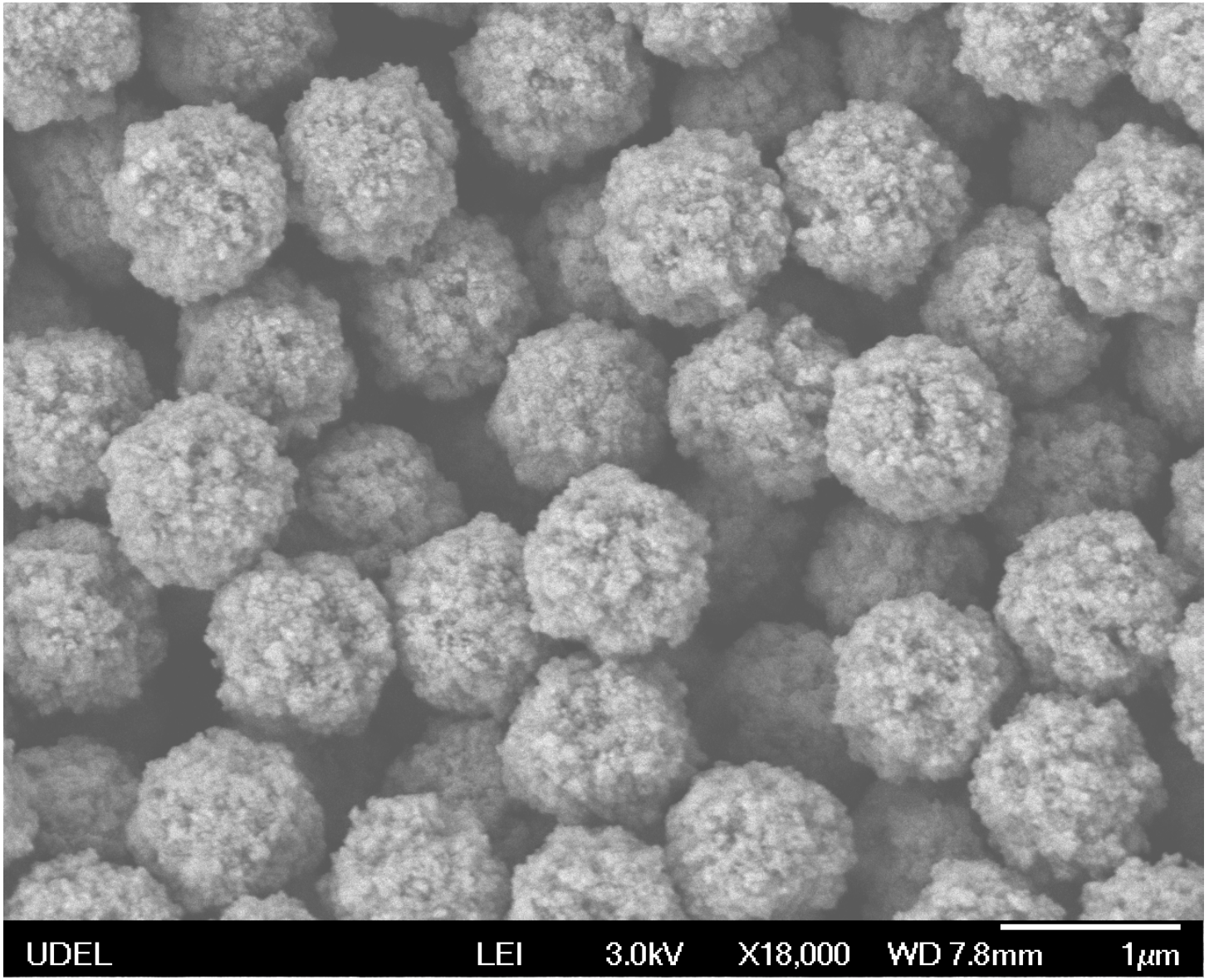

Arrested, gel-like structure

Magnetorheology & electrorheology

M. Fermigier and A. P. Gast,, *J. Colloid Interface Sci.* 154, 522 (1992).
R. T. Bonnecaze and J. F. Brady, *J. Rheology* 36, 73 (1992).
R. T. Bonnecaze and J. F. Brady, *J. Chem. Phys.* 96, 2183 (1992).

H-field
0.9A, 10 Hz

1.71×1.14 mm
Elapsed time: 1hr

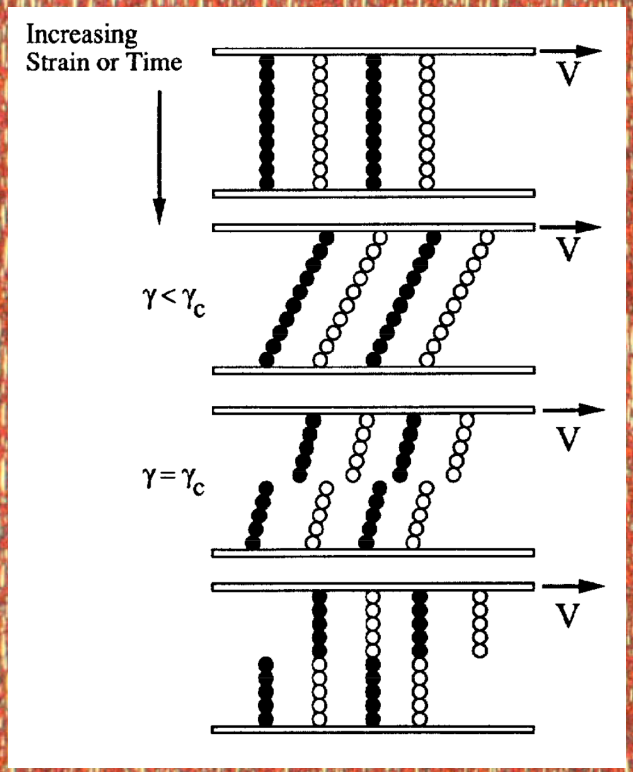

E. M. Furst—*CMET/Chemical & Biomolecular Engineering, University of Delaware*—furst@udel.edu

Toggled fields

$$\xi = \frac{t_{\text{on}}}{t_{\text{on}} + t_{\text{off}}}$$

0.1 – 0.8 duty fraction

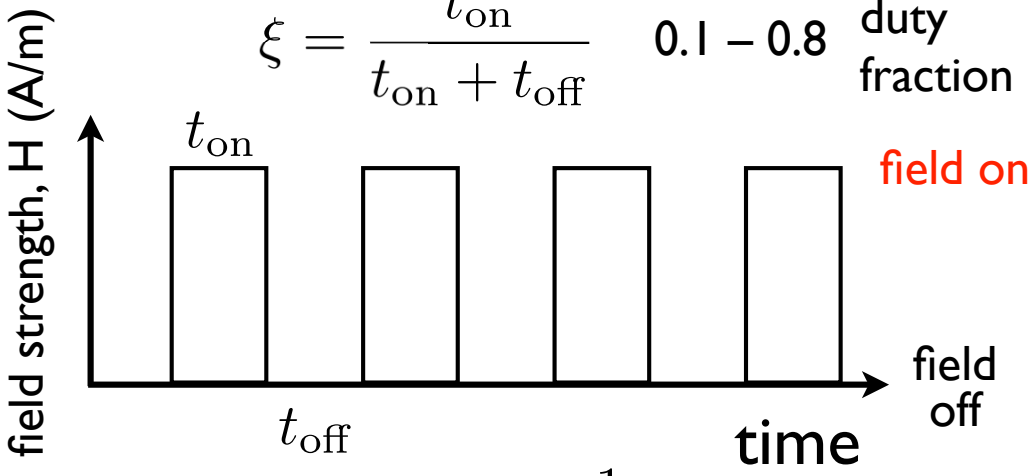

frequency 0.25–10 Hz

$$\nu = \frac{1}{t_{\text{on}} + t_{\text{off}}}$$

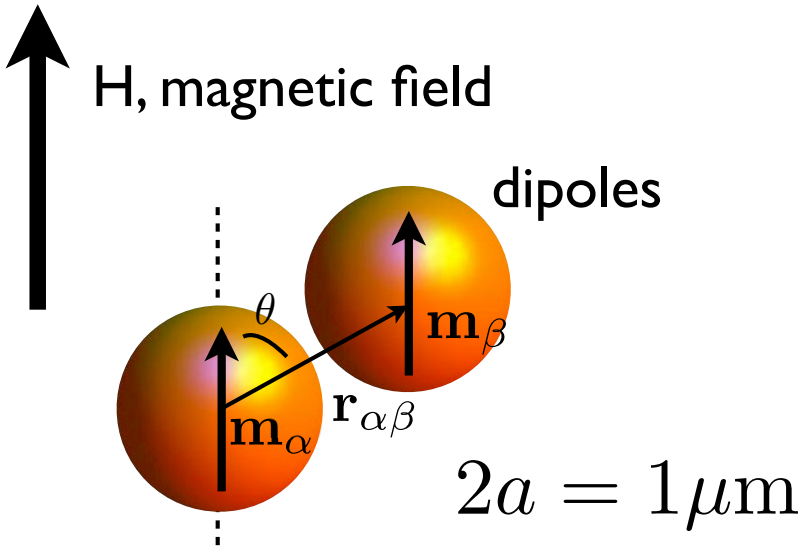

$2a = 1\mu\text{m}$

Field strength 600 – 2600 A/m

$$\lambda = \frac{\text{maximum attraction}}{kT} \sim 100$$

Volume fraction 5×10^{-3}

Magnetic colloids in toggled field, 0.66 Hz

Elapsed time: 1hr

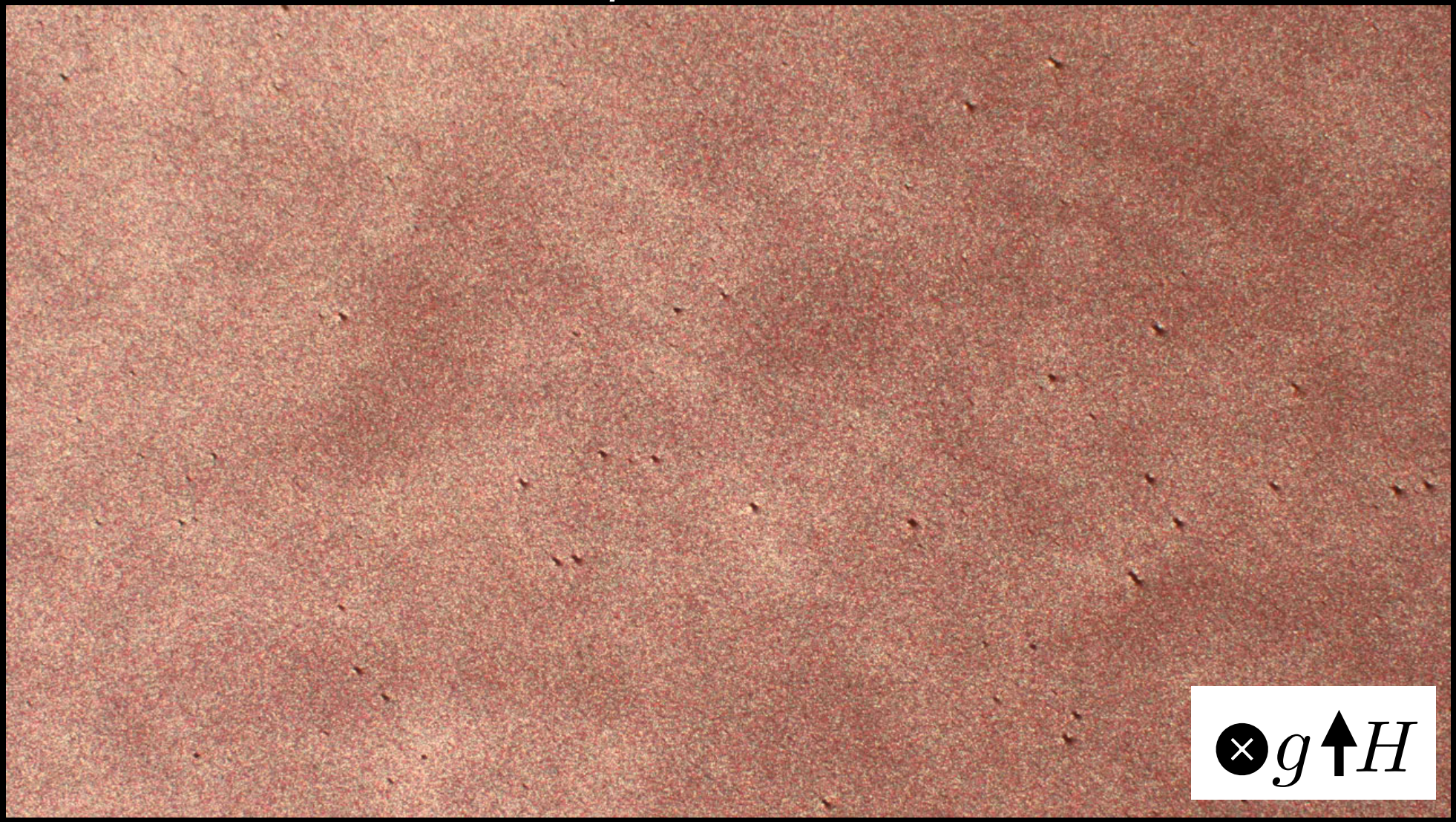

H-field 0.9A, 0.66 Hz, 0.5 duty

1.71×1.14 mm

Kim, H.; Sau, M.; Furst, E. M., *Langmuir* 2020, 36, 9926–9934.
Bauer, J. L., et al, *Langmuir* 2016, 32, 6618–6623.
Bauer, J. L., et al. *J. Chem. Phys.* 2015, 143, 074901.
Swan, J. W.; Bauer, J. L.; Liu, Y.; Furst, E. M. *Soft Matter* 2014, 10, 1102–1109.

Phase diagram of toggled sticky spheres

Z. M. Sherman & J. W. Swan, *ACS Nano* 10, 5260–5271 (2016).
Z. M. Sherman, et al. *Langmuir* 34, 1029–1041 (2018).

$\varepsilon = 10 k_B T$
$\phi = 0.2$

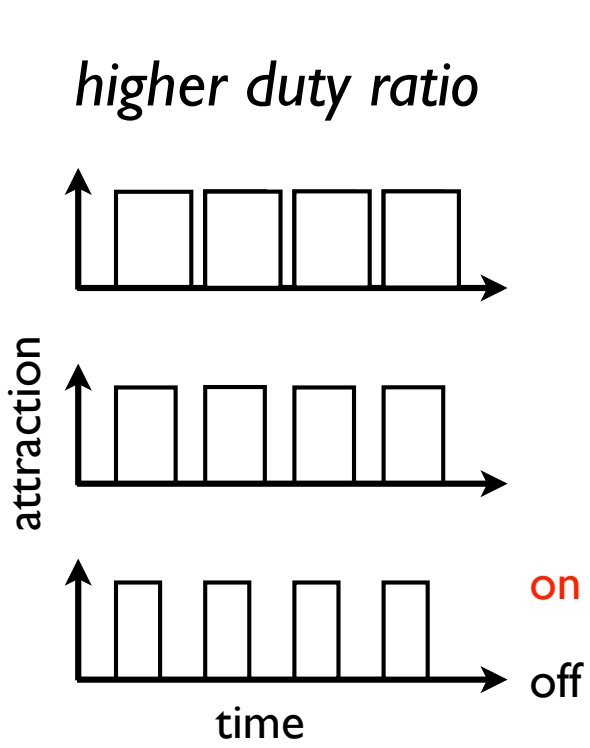

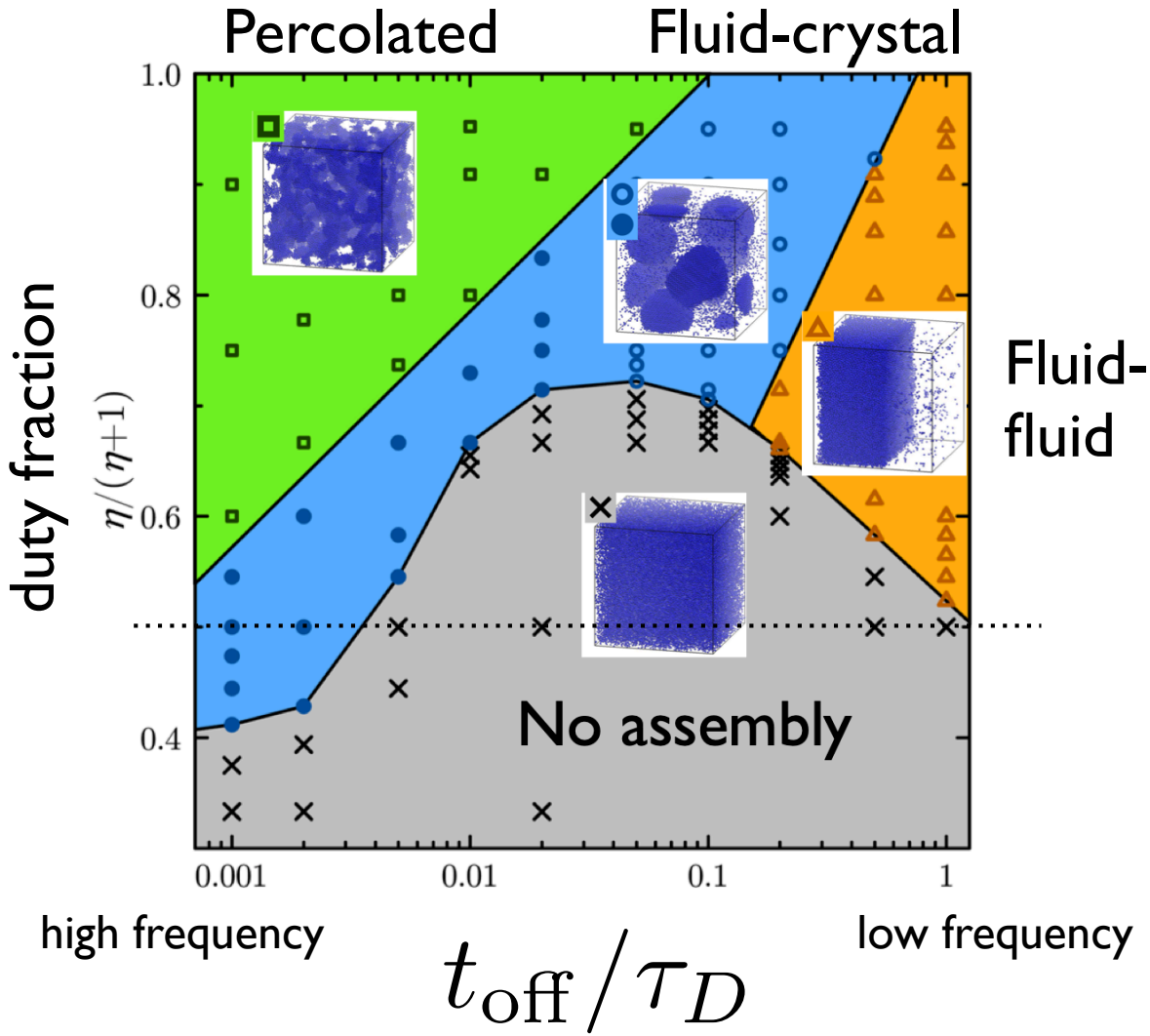

Phase diagram of toggled sticky spheres

Z. M. Sherman & J.W. Swan, *ACS Nano* 10, 5260–5271 (2016).
Z. M. Sherman, et al. *Langmuir* 34, 1029–1041 (2018).

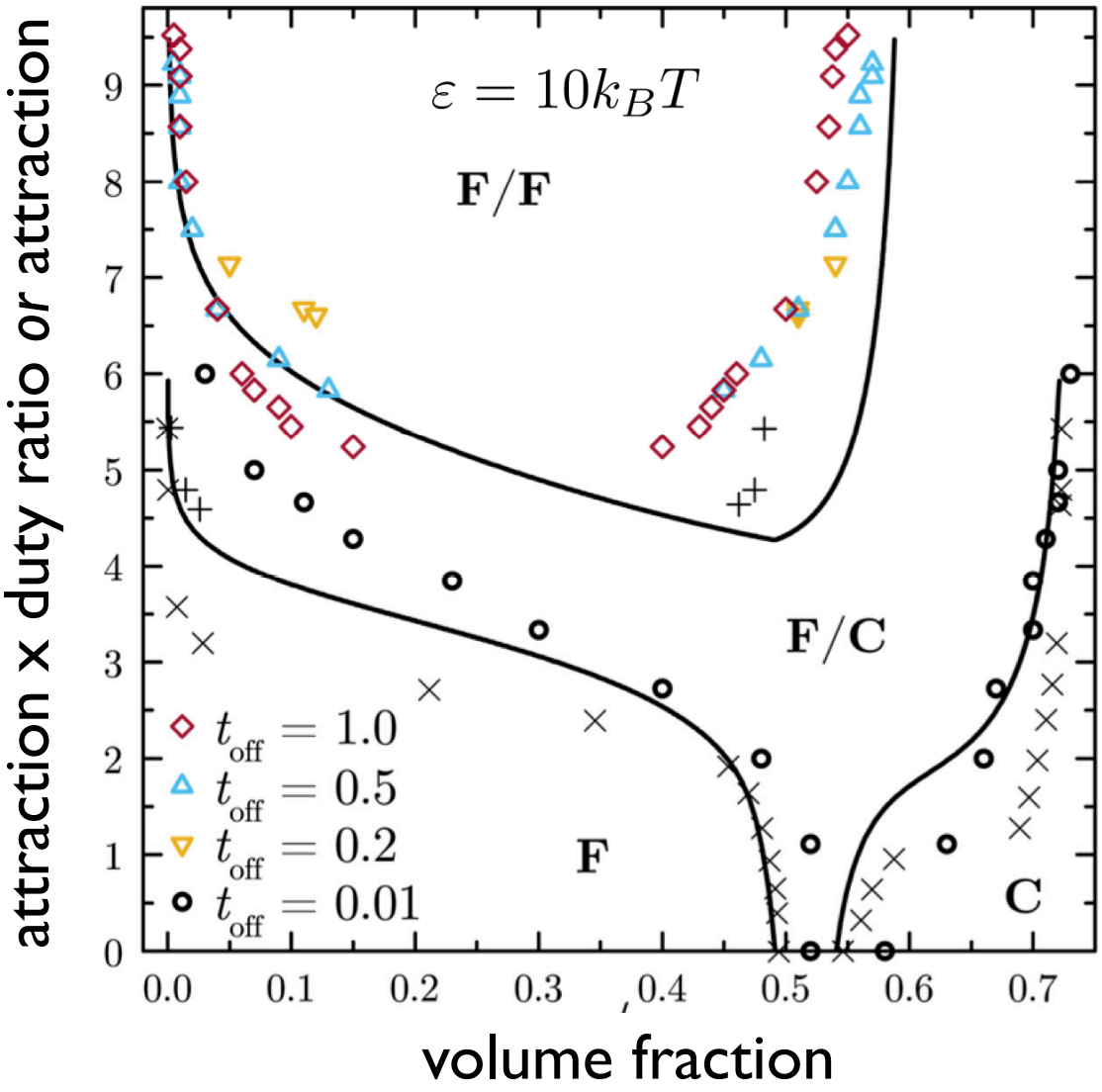

$$\bar{\mu}_{\text{I}}(\phi_{\text{I}}) = \bar{\mu}_{\text{II}}(\phi_{\text{II}})$$

$$\bar{P}_{\text{I}}(\phi_{\text{I}}) = \bar{P}_{\text{II}}(\phi_{\text{II}})$$

Time-averaged *P*, *μ*

$$\bar{X} = \mathcal{T}^{-1} \int_T X(t)dt$$

$$\mathcal{T} \equiv t_{\text{on}} + t_{\text{off}}$$

Time-averaged EOS

$$\bar{P} = P_{\text{HS}} + \frac{\eta\epsilon}{\eta+1} f(\phi)$$

$$\bar{\mu} = \mu_{\text{HS}} + \frac{\eta\epsilon}{\eta+1} g(\phi)$$

ϵ - attraction strength

Gel-like states of toggled sticky spheres

Z. M. Sherman & J.W. Swan, *ACS Nano* 10, 5260–5271 (2016).
Z. M. Sherman, et al. *Langmuir* 34, 1029–1041 (2018).
S. Ramakrishnan, et al., *Physical Review E* 70, 40401 (2004).
Z.Varga, G.Wang, and J. Swan, *Soft Matter* 11, 9009 (2015).

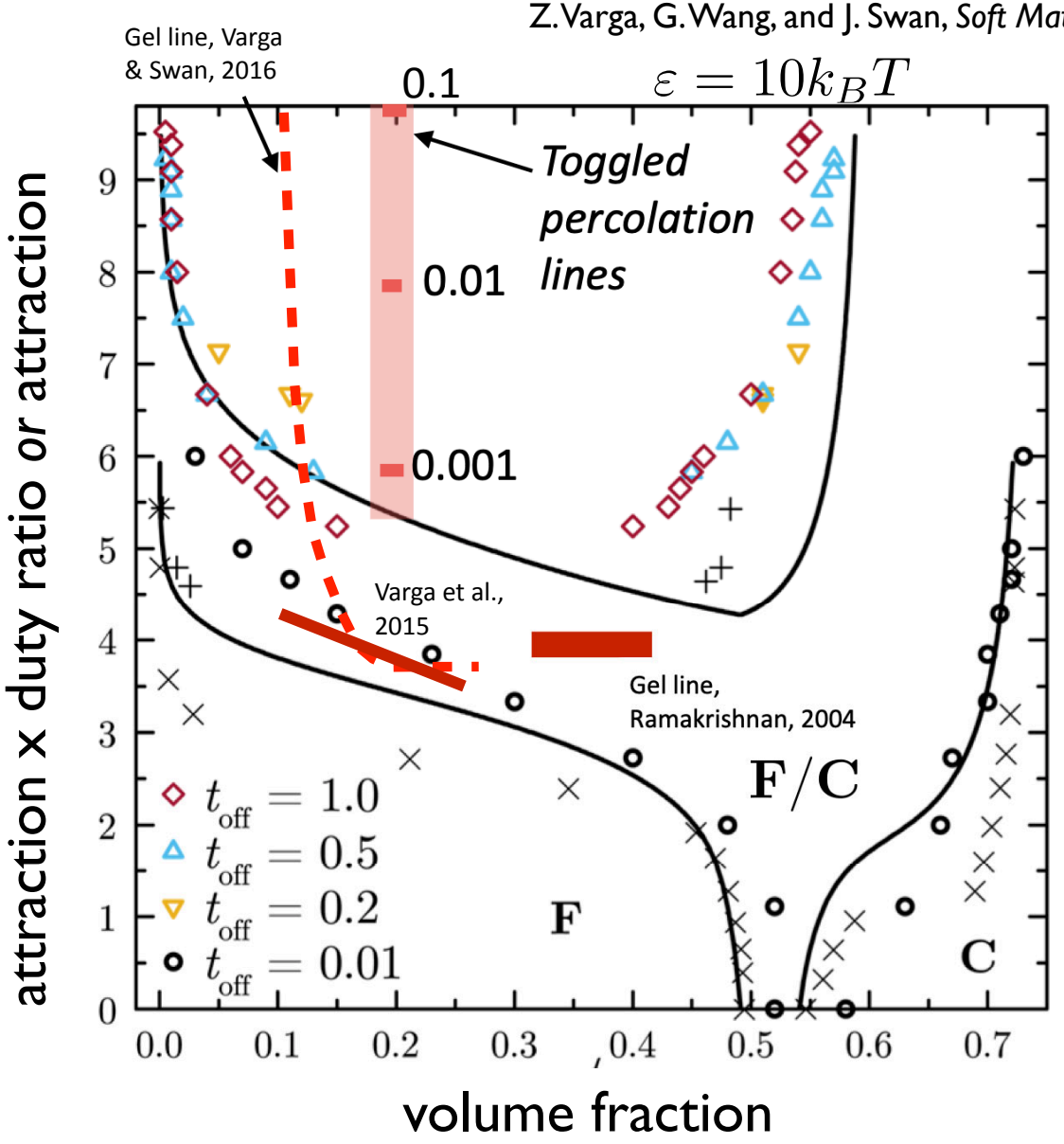

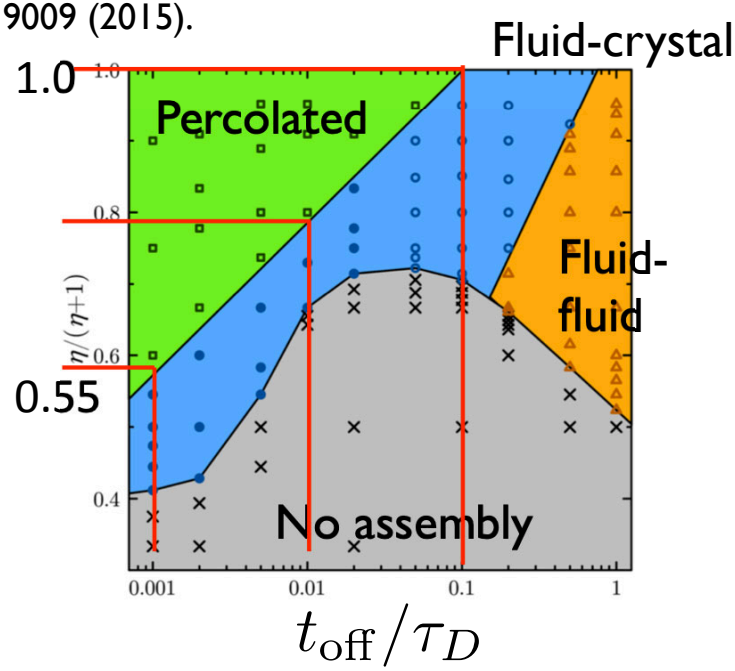

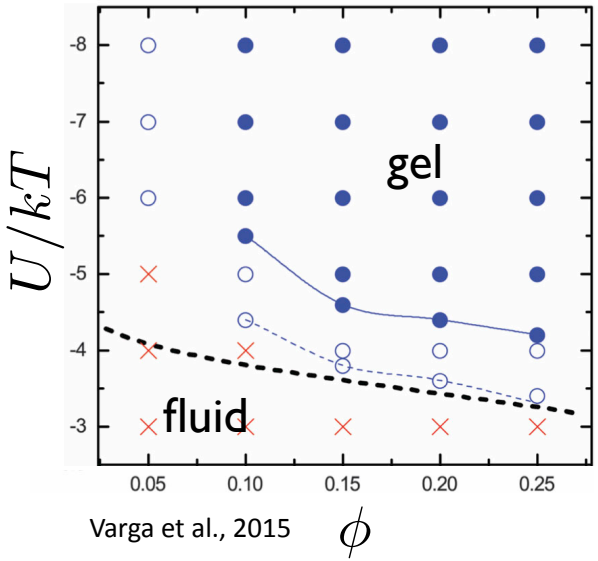

Concluding remarks

K. A. Whitaker et al., *Nat. Commun.* 10, 2237 (2019).
F. Bonacci et al., *Nat. Mater.* 19, 775–780 (2020).
F. Bonacci et al. *Phys. Rev. Lett.* 128, 018003 (2022).

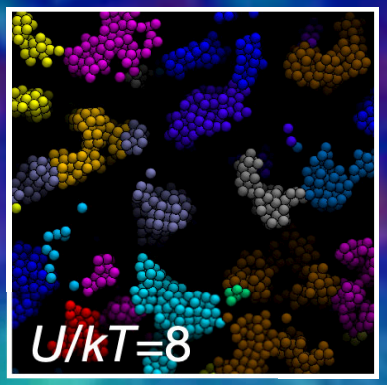

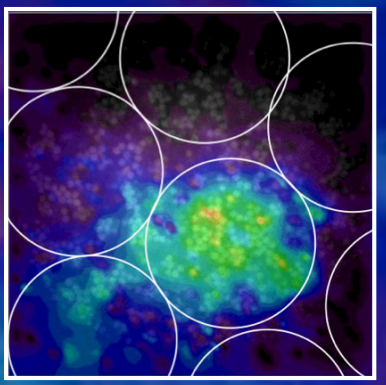

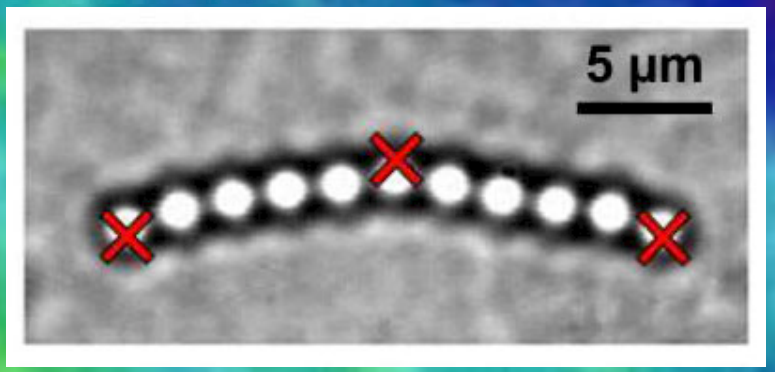

- Particle gels are ubiquitous but not universal
- Particle interactions drive structure and rheology
- Cluster gels: controlling formation of structure (e.g. annealing)
- Van der Waals gels: controlling surface chemistry
- What happens in driven (e.g. dissipative) assembly?